The forest transition and ecological thresholds: resilience, recovery, and predictions

by

Robert Gooding-Townsend

A thesis
presented to the University of Waterloo
in fulfillment of the
thesis requirement for the degree of
Master of Mathematics
in
Applied Mathematics

Waterloo, Ontario, Canada, 2018

© Robert Gooding-Townsend 2018

I hereby declare that I am the sole author of this thesis. This is a true copy of the thesis, including any required final revisions, as accepted by my examiners.

I understand that my thesis may be made electronically available to the public.

Abstract

A central topic in modeling land use change is to understand the "forest transition" from deforestation to net reforestation. Agricultural land use change is the main driver of this phenomenon; classically, agricultural land expands considerably to feed a growing population, and then declines as efficiency gains are realized, marginal farmland is abandoned, and rural populations move to cities. As a result, existing models have focused on the socioeconomic and demographic factors that drive agricultural intensification. However, in doing so, these models often neglect the role of ecological feedback effects and thresholds. These ecological thresholds can cause rapid shifts in ecosystems, such as forest collapse, based on small changes in parameters, and are very difficult to predict. The existence of these thresholds implies that agricultural expansion carries a risk of forest collapse. We aim to use realistic models to assess the risk of collapse in forest cover, dependence on key parameters, and strategies to avoid it.

To address the risk of forest collapse, we develop and analyze a differential equation model that incorporates both agricultural intensification and ecological thresholds. We use parameter values from the literature to adapt this model to boreal and tropical forests. We analyze the model with bifurcation diagrams, simulations of key resilience metrics, and fitted time series of real-world data for China, Costa Rica, and Vietnam.

Our analysis shows that there is a risk of forest collapse, and that the system is particularly sensitive to agricultural parameters. We find that regardless of the mechanism by which collapse occurs, there is a critical value of 20-25% forest cover. In scenarios of interest (i.e. forest transitions), initial deforestation would result in collapse if left unchecked. We estimate model parameters at multiple points along historical time series, which allows us to infer the risk of collapse and identify historical patterns. This shows that forest transitions can be caused by more varied parameter patterns than classically assumed in the literature; in particular, rates of land conversion and agricultural abandonment rate may remain elevated, instead of declining after intensification. The agricultural abandonment rate is a key advance predictor of collapse at long time horizons, but at the brink of a crisis forest collapse can best be avoided by reducing the forest conversion rate. We argue that ecological threshold effects should be acknowledged in forest transition models not only for ecological accuracy but also to ensure prudent forest management, particularly in the face of emerging risks such as climate change.

Acknowledgements

I would like to thank my supervisors, Chris Bauch and Madhur Anand, for their dedication, knowledge, support, and good questions. I would like to thank my fellow grad students, both in the Bauch lab and outside it, for their help, jokes, companionship, and helpful cynicism. I would like to thank Kate Beggs, my family, and all of my non-grad-school friends for their mix of support, tough love, and occasional bafflement throughout my thesis.

Table of Contents

List of Tables

List of Figures

Chapter 1

Background

1.1 The Forest Transition

1.1.1 Conceptual background

The forest transition refers to a change from net deforestation to net afforestation, or moving from forest loss to forest gain. The ecological, economic, and cultural importance of forest preservation is hard to overstate. As early as 1893, it was asserted that "the wholesale and indiscriminate slaughter of forests brings a host of evils in its train" [1]. Modern language would frame these benefits in terms of ecosystem services, carbon emissions, and biodiversity, while avoiding catastrophic shifts in ecosystems [2]. Where forest cover continues to decrease, achieving a transition is a necessary first step in meeting other conservation goals.

Agriculture is the main driver of deforestation, and conversely forest transitions are mainly driven by agricultural intensification and land sparing [3]. These are in turn caused by socio-economic and population subprocesses such as abandonment of marginal (e.g. mountainous, poor soil) agricultural land, technologically increased yields, decreasing rural population density and employment, imports of agricultural and wood products from abroad, and forest protection policies. While increasing populations are one key factor driving agricultural expansion and deforestation, yield increases have been high enough to allow forest transitions while meeting increasing food demands [4, 5]. In recent decades, these shifts have caused forest transitions in many countries in the global north. However, deforestation continues in many countries in the global south, such as Indonesia and Cameroon, largely driven by market demand abroad [5].

1.1.2 Previous models

Models of the forest transition primarily focus on agricultural intensification. An early example is Mather and Needle [3]. This presents a simple agent-based model of landowners optimizing agricultural production in a grid of cells with different productivities. From an initial state of randomly dispersed cultivation, agents redistribute their cultivation to more productive grid cells over time. In the process, they increase agricultural efficiency, abandon marginal farmland, and provide opportunities for forest to grow, thus leading to a forest transition.

Much research into the forest transition takes a very different approach to the one we are presenting in this paper. This includes work by geographers focusing on specific spatial patterns underlying individual forest transitions [6, 7, 8]. As a highly interdisciplinary research area, it also includes work by economists and social scientists, with research questions focusing on socio-economic and policy determinants of the forest transition [9, 10, 5, 11, 12, 8].

However, neither of these broad areas is aligned with the specific modeling approach we intend to take in this project. One paper that does is Pagnutti, Bauch, and Anand's "Outlook on a worldwide forest transition" [4]. This is a discrete time model of land use change to fit the food needs of the world population, while agricultural efficiency also increases. The question on a global scale is whether consumption (e.g. food waste) can decrease or production can increase (e.g. through biotechnology) sufficiently to limit the expansion of farmland and preserve forests [4]. The structure of this model involves five land states (forest, farmland, pasture, abandoned land, and urban land) and the transitions between them. We take a subset of these land states, and the transitions between them, as the basis for our model. However, there are considerable differences, which we will elaborate in Section 1.3.

Another forest transition paper that presents a very similar model is Satake & Rudel [13]. This has just three land states: forest, farmland, and abandoned land. Landowners respond probabilistically to incentives in choosing whether to deforest their land and plant crops. The authors discuss two different hypotheses for determining the value of forested land: the forest scarcity and the ecosystem services hypotheses. Under the forest scarcity hypothesis, the value of forest increases for economic reasons as forest cover decreases, due to lower supply. Under the ecosystem services hypothesis, environmental degradation accompanied by loss of forests means that remaining forests have lower value. The environmental degradation hypothesis matches more closely with the ecological approach taken in this thesis.

Satake and Rudel find that incentives for conservation are stronger when forest regeneration is slower (i.e. deforestation is less easily reversible), and when landowners place a higher value on the future (i.e. short term gains from selling forest products are less attractive). Under the forest scarcity hypothesis, rapid forest regeneration and high discount rates both act to destabilize the system, resulting in pronounced oscillations in forest cover (which are likely vulnerable to perturbations). Under the ecosystem services hypothesis, there is a bi-stability between high forest and widespread deforestation, since below a critical threshold it is no longer worthwhile for landowners to maintain any forest; the location of this threshold depends on the discount factor, forest growth rate, and other parameters. Since this paper, particularly under the ecosystem services hypothesis, is so similar to the present work, a more detailed comparison is given in Section 1.3.

1.2 Ecological thresholds

While environmental change is common to all ecosystems, some changes occur gradually, whereas others occur abruptly. These abrupt or "catastrophic" changes are generally the result of bistability, whereby alternative stable states coexist in a system [2]. Examples include lake eutrophication, desertification, and forest/grassland mosaics [2]. In all cases, these stable states and the shifts between them are due to feedback effects that either stabilize an existing state or accelerate the change to a new state [14].

Specifically, extensive data has been collected on thresholds between forest and grassland, especially within the context of savannah ecosystems. The clear demarcation and coexistence of these life forms (instead of one inevitably spreading into the other) perplexed a generation of ecologists, and became known as the "savannah problem" [15], and several feedback mechanisms are known. These include fire risk [16], soil retention [2], moisture capture, species composition, and other factors such as strong spatial interactions [17]. For the purposes of this thesis, we take a phenomenological approach to threshold effects. That is, we do not assume or explicitly model any particular mechanism; we only assume that some threshold is present for forest growth.

Ecological thresholds are often demonstrated by empirical patterns in tree cover distributions. Scheffer *et al.* demonstrate that tree cover in the earth's boreal region is multimodal, with clear thresholds between different vegetation regimes despite unimodal climactic conditions [18]. As a more detailed and mechanistic example, alternative stable states of spruce-lichen and spruce-moss forest types, and the importance of fire regimes and spruce budworm for inducing the changes between them, have been demonstrated in the boreal forests of Québec [19].

Analogous findings of clear thresholds and feedback mechanisms, particularly surrounding forests' ability to retain moisture or resist fire, have been found in tropical forests around the world. The nature and scale of these feedback effects is quite varied [20]. Hirota, Scheffer and colleagues show in a series of papers that the empirical distributions of tropical tree cover, and of response to shocks such as drought and deforestation, match closely to theoretical threshold models [21, 22, 23]. These papers are described in more detail below.

Within the field of (ecological) thresholds, a prominent subfield is concerned with predicting critical transitions. This typically involves monitoring small fluctuations of a system around its equilibrium, and using increasing autocorrelation to infer that a critical transition is imminent [24]. Though this methodology is standard and has been applied to a wide variety of systems, we will see that it turns out not to apply to our system of interest.

1.2.1 Previous models

Basic models of nonlinear growth are standard introductory material in mathematical ecology (e.g. [25]). One of the simplest models is the logistic equation (Eq. 1.1):

$$\frac{dx}{dt} = rx(1 - \frac{x}{K}) \tag{1.1}$$

This equation represents constrained growth, with population size x (assumed to be nonnegative), fecundity r, and carrying capacity K. This equation has two equilibria: $x = 0$ and $x = K$, corresponding to zero population or a population at carrying capacity. The $x = 0$ equilibrium is unstable, while $x = K$ is stable, meaning that as long as there are some individuals present, the population will grow towards the carrying capacity, at a rate determined by r. The growth rate is largest at $x = \frac{K}{2}$.

This simple model is useful in some situations, but fails to capture key aspects of some organisms' population dynamics. In many species, the population will die out if there are too few individuals. This can arise from difficulty finding a mate, vulnerability to predators, or other factors. This is called a **strong Allee Effect**. (In a weak Allee effect, the growth rate at low population densities is only slowed, instead of becoming negative.) It can be modelled as:

$$\frac{dx}{dt} = rx(\frac{x}{A} - 1)(1 - \frac{x}{K}) \tag{1.2}$$

The new term A $(0 < A < K)$ is the Allee threshold. Below this value, the population will decline to zero; above this value, it will increase up to the carrying capacity as in logistic growth.

Mathematically, critical thresholds are a (rather introductory) part of bifurcation theory [26]. However, since we are just concerned with a simple cusp bifurcation in an ecological context, the topic is usually sufficiently covered in introductory books on mathematical biology [25]. We will focus on specific models pertaining to ecological forest models.

In this thesis, we will focus on two forest types: boreal and tropical. Boreal forests were chosen because of their large area [27] and relevance to Canada. Tropical forests were chosen because of the importance in the context of the global carbon cycle and biodiversity, and because they are the most threatened [10]. In particular, considerable deforestation is ongoing in many tropical forests, and thus they should be a priority for achieving a forest transition [5].

Some previous models are not restricted to a particular forest type. One simple model of threshold-based forest growth is described by Innes, Bauch, and Anand [28]. This models the growth of forest F as a logistic equation with a threshold function $w(F)$

$$\frac{dF}{dt} = w(F)F(1-F) - bF \tag{1.3}$$

The function $w(F)$ is a sigmoid that ensures very low growth below 40% forest cover, and normal logistic growth above this level up to the carrying capacity. In their model, this forest growth is coupled to a social feedback mechanism representing human attitudes to forest conservation. No such coupling is included in our model, but we have adopted the same terminology for the sigmoidal growth function.

There are a number of models of ecological thresholds within the context of tropical forests. Staal *et al.* [23] also use a modified logistic growth function (Equation 1.4).

$$\frac{dF}{dt} = r(P)F\left(1 - \frac{F}{K}\right) - m_A F\frac{h_A}{F + h_A} \tag{1.4}$$

In this equation, $r(P)$ is a moisture-dependent fecundity term, K is the carrying capacity, m_A is the magnitude of Allee-effect mortality, and h_A is the Allee threshold. In this model, unlike Equation 1.3, it is the mortality term that is threshold-based and not the growth term. In practice, however, the dynamics are very similar. Previous models by the same research group [21, 22] established that these threshold-based dynamical models fit the data on tree cover distributions reasonably well. The version presented by Staal *et al.* was formulated to answer a research question about the combined effect of drought and deforestation. The moisture-dependent growth rate is necessary to investigate the effects of drought, and they model deforestation as a simple one-time decrease in forest cover.

There are relatively few differential equation models of boreal forest dynamics in the literature. One of the few is Henderson, Bauch, and Anand [29]. Chapter 2 of this thesis reviews empirical models of various recruitment functions, with mechanisms such as sapling recruitment, biomass growth, water stress, and fire risk. In Chapter 3, a model is developed to model the dynamics of the boreal forest in eastern British Columbia. This model, which is in part calibrated with the data from Scheffer *et al.* described above ([18]), has a similar functional form to Equation 1.3, with additional terms to account for drought-based mortality, harvesting, replanting, and probability of tree establishment. The forest growth function we will use is simpler (Chapter 2), in that these factors are assumed to be incorporated endogenously in model parameters.

1.3 Rationale and Objectives

The central goal of this thesis is to include threshold-based forest dynamics in a model of an intensification-driven forest transition. (Models which accomplish similar goals are described below, but I argue that none has accomplished precisely this goal.) Furthermore, the present approach is unique in analyzing this phenomenon with such a simple model. This allows a clear analysis of the interaction of agricultural intensification and ecological thresholds.

Many of the initial efforts in coupled socio-ecological models referenced above only qualitatively describe the dynamics of interest (beyond the qualitative similarity captured by initial models of socio-ecological systems [30, 13, 28]). We seek to address this by both setting parameter values as realistically as possible from prior literature (Table 2.1) and by demonstrating the model fit for real-world examples of forest transitions (Chapter 4).

Several prior authors in the forest transition literature have included ecological feedbacks in models of the forest transition. Satake and Rudel's model [13], as described above, considers the same three basic land uses and dynamics as ours. Under their ecosystem services hypothesis, the feedback effect they consider is quite similar to the ecological thresholds discussed above. (Although their density-dependent growth is linear rather than sigmoidal, this difference is fairly minor.) However, their model is purely conceptual, and not parameterized with real data. Our forest dynamics in the absence of human intervention are slightly more sophisticated, with flexibility in parameter values to account for natural forest-open land bistability. In addition, changes in forest conversion and farmland abandonment are left as exogenous in our model; without Satake and Rudel's explicit social coupling, we are more free to explore arbitrary shifts in these key parameters, which correspond to more macroeconomic changes as compared to the microeconomics of their

social model. We also add an element of prediction, in providing tools to detect potential forest collapses from data before they occur. The main difference between the present work and Satake and Rudel's paper is the inclusion of more ecological realism and data.

By contrast, the difference when compared to Staal, Decker, Hirota, and Nes 2015 [23] is a more detailed consideration of agriculture and of forest transition literature. Staal *et al.* use a well-calibrated, ecologically sophisticated model of forest dynamics to determine the combined effects of drought and deforestation on the Amazon forest. However, this approach models deforestation only as an impulsive shock (instantaneously reducing the forest cover by e.g. 20%). Considering the fact that conversion to agriculture is the leading cause of deforestation [31, 11], we extend this line of inquiry by considering the full dynamics of agriculture as a land use. How much forest is taken out of circulation, and at what rate does existing farmland become abandoned and re-wilded? The forest transition literature, and our macro approach of focusing on net conversion rates, offers a framework for answering these questions.

This thesis is grounded in the literature on forest transitions and on ecological thresholds, and will focus on understanding, interpreting, and avoiding collapses in forest cover. Specifically, my objectives are:

1. To develop an empirically grounded model of forest dynamics incorporating both ecological thresholds and land use intensification;

2. To examine the theoretical implications of ecological thresholds in forest transition scenarios, focusing on the potential for forest collapse;

3. To analyze and weigh risk factors for forest collapse, particularly those under human control.

The model is developed and parameterized in Chapter 2. Its theoretical properties – equilibria, bifurcations, and metrics of resilience and recovery in forest transitions – are analyzed in Chapter 3. In Chapter 4, the model is applied to real-world data in two different ways, with parameters varying over time either continuously or discretely; in each case, comparisons are made to theoretical results of Chapter 3, and sensitivity to key land use change parameters is discussed. Overall conclusions, limitations, and directions for future work are discussed in Chapter 5.

Chapter 2

Model

2.1 Model description

The model describes three land types: forest (F), agricultural land (A), and open land (G for 'Grassland'). Open land is a broad category encompassing natural grasslands, pasture, abandoned cropland, and forest blowdown. The state variables of the model are the land areas of each class, represented as proportions. The inclusion of just three land cover classes is a significant assumption, as it neglects dynamics of urbanization, water and wetlands, and finer distinctions within these three classes (e.g. forest composition or crop types). Where urban development or other land use classes are significant but constant throughout the study period, we can simply renormalize to the undeveloped land and recover the situation described above. This seemingly broad assumption holds for 38 out of 46 US ecoregions for which data is available [32].

Forest is subject to three processes: growth, natural loss, and conversion to farmland. Growth is logistic, and is proportional to current forest cover, available open land, and a density-dependent fecundity function $w(F)$. Natural disturbance to open land, through fire and storm blowdown, occurs at a constant rate b. Conversion to agricultural land occurs at a rate $u(t)$. Like other human-determined parameters, this conversion rate varies over time.

Agricultural land increases by conversion of forest and open land and decreases by abandonment. Conversion of forest was described above; conversion of open land is analogous, with rate $v(t)$. We assume that in general $v(t) > u(t)$, as it requires more effort to clear forest than to prepare open land for agriculture. Farmland abandonment occurs at a

rate $\gamma(t)$, with abandoned farmland becoming open land; this includes temporarily fallow fields as well as permanent abandonment. In situations with rapid turnover of farmland, such as shifting cultivation [33], both farmland abandonment rates and land conversion rates will be high.

The processes affecting open land have already been described: it increases by natural disturbance of forests and abandonment of agricultural land, and decreases by forest growth and conversion to agriculture.

The system of model equations is as follows:

$$\frac{dF}{dt} = w(F)GF - bF - u(t)F \tag{2.1}$$

$$\frac{dA}{dt} = u(t)F + v(t)G - \gamma(t)A \tag{2.2}$$

$$\frac{dG}{dt} = -w(F)GF + bF + \gamma(t)A - v(t)G \tag{2.3}$$

Since total land area is constant, we normalize it to 1. This allows us to eliminate the redundant equation for G (Eq. 2.3), which we replace by $G = 1 - F - A$.

', $\propto G$, forest con-
imply a relatively

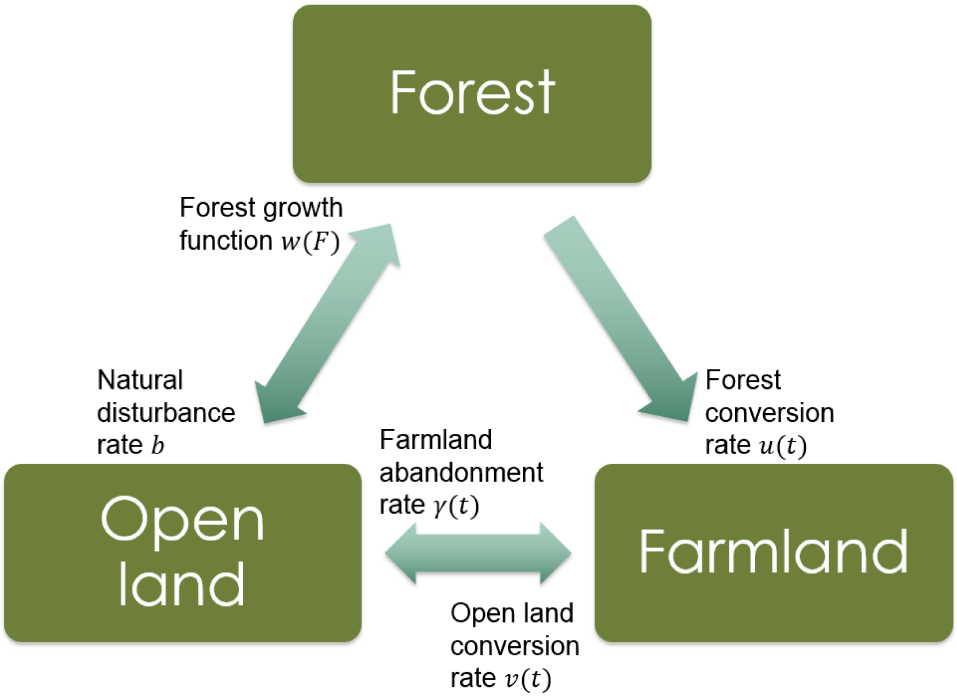

Figure 2.1: The three land classes and associated conversion rates.

well-mixed system, where land use change is occurring in small patches. This assumption is consistent with patch-based models [3] and previous differential equation formulations [29, 13]. In some cases, these choices of proportionality have additional interpretations: for example, forest conversion may become more difficult at low densities if the remaining forest is increasingly inaccessible. The proportionality of farmland abandonment implies that $1/\gamma$ is the average lifetime of a farm. These choices also help ensure the model stays well-defined: areas land areas cannot become negative.

Table 2.1: Parameter definitions, ranges, and sources

			Boreal		Tropical		
Term	Meaning	Units	Range	Baseline	Range	Baseline	Sources
a	Low-density forest growth rate	% area/y	0-2	0	0-10	0	[29, 22]
b	Natural disturbance rate	% area/y	0.5-2.5	1.0	1-26	2.5	[29, 22, 23, 34]
h	Threshold for increased growth	% area	5-60	15	5-50	15	[29, 35, 18, 23]
p	Hill function steepness (range)	–	2-7	3	2-7	3	[29, 18, 23]
r	High-density forest growth rate	% area/y	2-10	9	10-50	27	[29, 18, 23], derived
$\gamma(t)$	Farmland abandonment rate	% area/y	0-6	1.5	0-25	8	[9, 36, 37]
$u(t)$	Forest conversion rate	% area/y	0-5	0.4	0-25	2	[4, 38, 27]
$v(t)$	Open land conversion rate	% area/y	0-8	1.2	0-50	6	[36, 4]

2.1.1 Forest growth function

As mentioned previously, the fecundity function $w(F)$ is density-dependent. This is the mechanism by which ecological feedbacks and thresholds are represented in this model. We parametrize this as a Hill function with a low-growth regime and a high-growth regime, as in [22, 23].

When forest cover is low, are in the low growth regime, at rate a. At high forest cover, the model switches to a high growth regime, with an increase in growth rate of magnitude r.

The transition between the two regimes is parameterized by a Hill function with steepness parameter p and a half-saturation forest cover h (Equation 2.4), as illustrated in Figure 2.2.

$$w(F) = a + r\frac{F^p}{h^p + F^p} \tag{2.4}$$

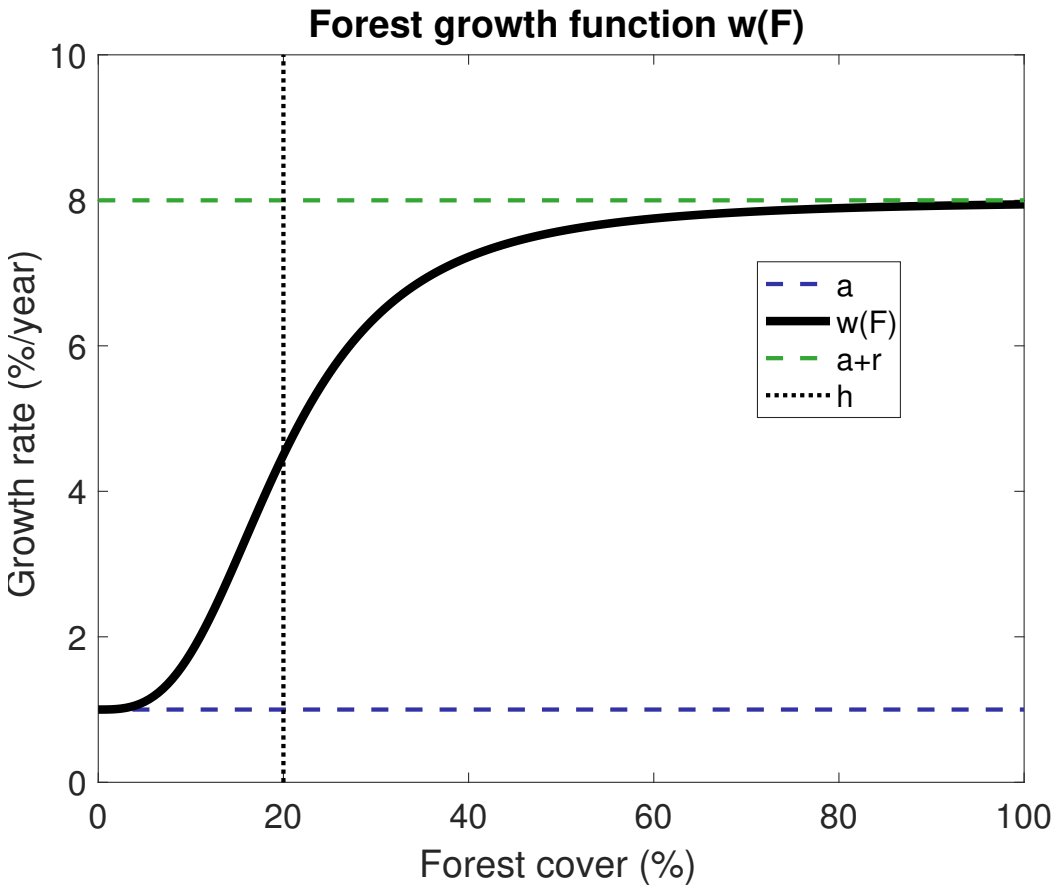

Figure 2.2: The density-dependent forest growth function $w(F)$.

Note (Table 2.1) that the baseline value of a is 0, which suggests this parameter may be redundant. However, the reason we retain it is that a acts as a "switch" for stability of the $F = 0$ equilibrium: when $a < b$, $F = 0$ is a stable equilibrium. Since there is also an interior equilibrium under low agricultural pressure (Sec. 3.1), this ensures that our system

is able to reflect the bistability between forest and grassland [16]; however, by increasing a, we can also ensure monostability, thus reflecting climactic conditions in which forest is the only stable outcome.

2.1.2 Natural versus human parameters

Throughout this work (e.g. on Table 2.1), we refer to two distinct sets of parameters: the natural parameters and the human parameters. The **natural parameters** $\{a, b, h, r, p\}$ are those that affect transitions between forest and natural open land; the **human parameters** $\{\gamma, u, v\}$ are those that affect transitions to and from agricultural land. There are two important reasons for making this distinction: timescale, and ability to affect change.

We expect that the human-influenced parameters vary quite rapidly, often on the order of years. This is because land conversion is tied to multiple economic, demographic, technological, social, and technological processes that vary on these timescales [9, 27, 37]. The frequent occurrence of such rapid changes in parameter values is why these parameters are listed as functions of time. ("Rapid" is in relation to the timescale for the model to reach equilibrium, which is often more than 100 years.) In this work, two approaches are used for modeling this variation in time. The first approach, for simulation, is of a smooth transition between an initial value and a final value (Chapter 3); the second approach, for working with real-world data, is to generate an ensemble parameter estimates based on updated data every 5 years (Chapter 4).

The second reason for this separation is that the human parameters are much more directly under human control. Due to massive coordination problems and the magnitude of socio-economic forces involved, it may be impossible for any single agent to directly change land conversion rates. However, agriculture is undeniably under human control. Further, a number of policy initiatives, such as agricultural subsidies and payment for ecosystem services, have been shown to effect land use behaviours. One of the goals of the present research is to consider which possible interventions (in γ, u, or v) best achieve conservation goals in various circumstances.

Although the human parameters change quickly and are at least in principle controllable, it is important to note that these properties may also hold to some extent for natural parameters. For example, climate change may alter the high-density forest growth rate r, causing it to increase in some areas and decrease elsewhere [39, 40]. Climate change will also increase the frequency and severity of fires and droughts, as represented by the natural disturbance rate b. Other natural parameters, such as the steepness p and half-saturation h of the Hill function, may vary with species composition. The underlying biotic and abiotic

factors determining the "natural parameters" of this model will change over time, though the relevant timescale is more likely to be decades or centuries. And while they are not entirely governed by human actions, as agricultural land use is, the natural parameters can be affected in multiple ways by human activity. This could be direct, such as tree planting to increase the low-density growth rate a, or indirect, such as altering species composition.

2.2 Parametrization

Following our objective of developing an empirically grounded model, we determine all parameter values from established literature. The details (and difficulties) are described in the following section; Chapter 4 also discusses fits to real-world data.

As shown on Table 2.1, we adapt the model to describe two distinct settings: tropical and boreal forests. Parameters for each are calibrated based on published literature and available data, as described below. As this is a general model, specifying point values for parameters would be inappropriate, as this would not capture the range of variation within each forest type. We use the lower bound, estimated peak (i.e. the most probable or typical value), and upper bound to define triangular distributions for each parameter, which form the basis of our ensemble simulations (Sec. 3.4). Sensitivity analysis at baseline, shown through bifurcation diagrams (Figures 3.2-3.9), reveals that uncertainty in parameter values would not substantively change any of the model behaviour. Parameter values may appear very high, but this is because this model describes gross changes, which may often be more than an order of magnitude larger than net land cover changes in realistic settings [41].

In many cases, it is difficult to estimate parameters precisely. This is largely because the parameters in this model, while ecologically meaningful, do not often correspond to other researchers' questions of interest. This is particularly true of the constituent parameters in the Hill function. In cases where prior research does investigate density-dependent feedbacks on forest growth, it is typically within a mechanistic context of a particular phenomenon: fire risk [22, 28], fragmentation [23], and/or moisture retention. The present 'generic' model is phenomenological and does not distinguish the cause of density-dependent feedbacks; this resembles cases where frequency distributions and input variables suggest threshold effects but no mechanism has been firmly established [18]. This phenomenological basis is another reason our parameter estimates emphasize broad ranges over point estimates.

2.2.1 Low-density forest growth rate a

This represents the forest cover from 0; it is the intercept of the growth rate function $w(F)$. Most models of feedback effects do not include this term (e.g. [29][Ch. 2], [28]), thus implicitly setting it to 0. Further, a is difficult to find empirically since forest is only rarely introduced to completely deforested areas. Fortunately, at the baseline value, we find little sensitivity to a.

In light of these difficulties, it is worth examining why we include this parameter at all. The reason is that it acts as a switch for the bistability dynamics. If $a < b$, the $F = 0$ steady state is stable; for $a > b$ it is unstable. Because we are interested in bistability, we impose the condition $a < b$, even if in fact many global forests may not be in a bistable regime. For model simplicity, and ease of parameterization, we set $a = 0$, though we still estimate plausible ranges.

For managed boreal forests, Henderson reports a planting rate of $0.1\% \leq a \leq 0.6\%$ annually [29]. However, the growth rate from 0 is not just the planting rate: it also depends on the natural regeneration rate at $F = 0$, which reaches as high as approximately 2% annually. For tropical forests, we estimate $0 \leq a \leq 10$ % annually. Unfortunately, due to a lack of previous models, this is only an estimate; it is based on the approximate $a : r$ ratio in boreal forests.

2.2.2 Forest mortality b

Forest mortality includes losses due to storms, fire, and other natural processes. There are many reliable estimates for this parameter.

In tropical forests, annual loss estimates include 1% [42], 2% [29, Chapter 2]. Some models have much higher loss rates of 10-15% annually [23, 29] or even 26% [22] for very low tree covers, due to the combined effects of both fire-induced mortality and an Allee threshold. These very large loss rates do not reflect net loss, however, since they are balanced by greater growth rates in this model (and the present model reduces the growth rate at low F values, rather than increasing the loss rate).

For boreal forests, [34] gives a range of 0.5-2% for fire mortality, which agrees closely with the range of 0.5-2.5% reported in [29].

2.2.3 Sigmoidal threshold h

Direct evidence for the threshold value in forest growth is quite scant; we often infer the location of thresholds from the frequency distributions of forest cover [18]. Further, it varies considerably depending on the ecosystem, and in may cases there are multiple thresholds. We will report all threshold values, but for this research we are primarily interested in the lowest ones, between presence and absence of forest.

For tropical forests, thresholds have been reported at 10% and 64% [22], 20% and 70% [23] (inferred from frequency distribution;), and 40% [29, Chapter 2]. For boreal forests, Scheffer and colleagues' global survey reveals thresholds around 10%, 30%, and 60% [18]; Henderson and colleagues report a value of 25%, though it may range from 5-50% [29, Chapter 3]. We expect that thresholds occur at very low values in temperate forests as well, at least for national-scale forest cover, since countries such as France have experienced forest transitions at 14% cover [35], implying a threshold at most this large.

While this 'generic' system necessarily has a great deal of uncertainty in the location of the threshold, we are mainly concerned with the lowest threshold present, marking the collapse of the forest. In addition, sensitivity analysis shows that the dynamics are not very sensitive to this parameter.

2.2.4 Sigmoidal steepness p

Models based on fire risk have quite steep thresholds, with the exponent p as large as 7 [22] for fire risk in tropical forests. However, in this model the exponent for growth-dependent mortality (the Allee effect term) is 1.

For boreal forests, we have no direct estimates of steepness parameters. Instead, we estimate p from the frequency distribution in [18]. Since it is fairly shallow, we expect p to be approximately in the range of 1-5. This agrees qualitatively with the threshold response in [29, Chapter 3].

2.2.5 High-density forest growth rate r

This parameter governs the maximum expansion rate of forest cover, and as such is extremely important. It is also very well documented in previous logistic models of forest growth, and more generally in trends of forest cover area (though deriving the appropriate r value from forest cover area requires normalizing for both current forest and open land).

For tropical forests, estimates of r are often given as moisture-dependent in other models. For simplicity, we do not explicitly consider this variable; we simply incorporate high and low moisture regimes into our estimates for the range of r. Furthermore, the effect is only significant for very low precipitation levels. Published estimates of r include 10-50% [29] and 30% annually [22, 23] at high precipitation levels. However, to account for the moisture dependence, we reduce this by 10% to 27% annually.

For boreal forests, Henderson gives an estimate of 2-6% annually (depending on moisture and species). We can check this range from the steady state forest cover, using the relation $\bar{F} = 1 - b/(a + r)$. Since $\bar{F} \approx 80\%$, $b \approx 1 - 2\%$, and $a = 0$, this confirms that $r \in [5 - 10\%]$.

2.2.6 Farmland abandonment rate γ

In the tropics, shifting cultivation is frequently practiced. Under this regime, farmland can be left fallow after just 4-6 years [33], implying $u \in [16 - 25\%]$. Note that this is not technically abandonment, as landowners continue to use it for secondary crops and intend to return to growing primary food crops after a suitable period of time; however, for the purpose of this model, we count this fallow land as open. In tropical agriculture where shifting cultivation is not practiced, all transition rates, including abandonment, will be substantially lower. In cases where agriculture is profitable, land abandonment can be arbitrarily close to 0 (and in fact this occurs more often than might be expected [9]).

For boreal forests, an upper bound on the observed rates of farmland abandonment was provided from the breakup of the Soviet Union and its associated agricultural subsidies. This maximal rate is 2-6% annual abandonment [37].

2.2.7 Forest clearing rate u

We cross-reference this parameter from a number of sources. Many sources give estimates on the fraction of farmland derived from forest versus farmland; [4] gives this ratio as 2:3 globally. Hansen and colleagues provide data on overall ratios of forest loss to forest gain, which are about 3.6 for tropical forests and 2.1 for boreal forests [27]. In model terms, this means $b + u = 3.6 * w(F) * (1 - A - F)$; thus, $u \in [3 - 25\%]$. However, if people are not actively clearing forests, u may reach 0.

For boreal forests, the same calculation yields $u \in [1 - 5\%]$. Alternatively, we may use Popatov's finding that natural disturbance accounts for about 45% of forest losses in

their study area on the Northern Hemisphere [38]; this implies $u \approx 1.1b$, giving a similar range. However, these measurements were made in circumstances with declining forest cover. In post-forest-transition regions, where forest cover is stable, the forest clearing rate is substantially lower, reaching as low as 0.2% in Canada [43].

2.2.8 Grassland clearing rate v

We cross-reference this parameter indirectly, since it is hard to find existing estimates. Pagnutti and colleagues provide the fraction of farmland derived from forest versus grassland; [4] gives this ratio as 2:3 globally; hence $v > 1.5 * u$. (The inequality is because there is typically much more forest than grassland, so we have to rescale). However, this ratio may be as high as 4:1 in the tropics [36]. It is generally easier to farm grasslands than forests, so we would expect v to be quite high; however, if u is in the upper end of its range, it will be unfeasible to keep such high v values.

Chapter 3

Model analysis and simulation results

In this chapter the model is analyzed, with equilibrium analysis, bifurcation diagrams, and simulation results. The bifurcation diagrams offer a classical dynamical systems analysis, which comprehensively describes the behaviour of the system over a wide range of parameter values, such as might be found in different forest types or agricultural regimes. The simulations feature time-varying parameters to characterize land use intensification, which introduces inhomogeneity, with consequences that cannot always be described by bifurcation diagrams. In particular, during forest transitions multiple parameters are likely to be changing simultaneously, and they are changing at approximately the same timescale as the system dynamics. As a result of these issues, transients are key to our analysis [44], particularly for the real-world situations discussed in Chapter 4. First, however, we consider equilibria, typical trajectories, and bifurcations. We examine how both the initial parameters and the changes associated with land use intensification affect measures of forest resilience and recovery.

3.1 Equilibria and stability

3.1.1 Forest dynamics in the absence of agriculture

In an undisturbed system, the only land classes are forest and natural open land. Due to conservation, this can be modelled with the single equation:

$$\dot{F} = w(F)F(1-F) - bF \tag{3.1}$$

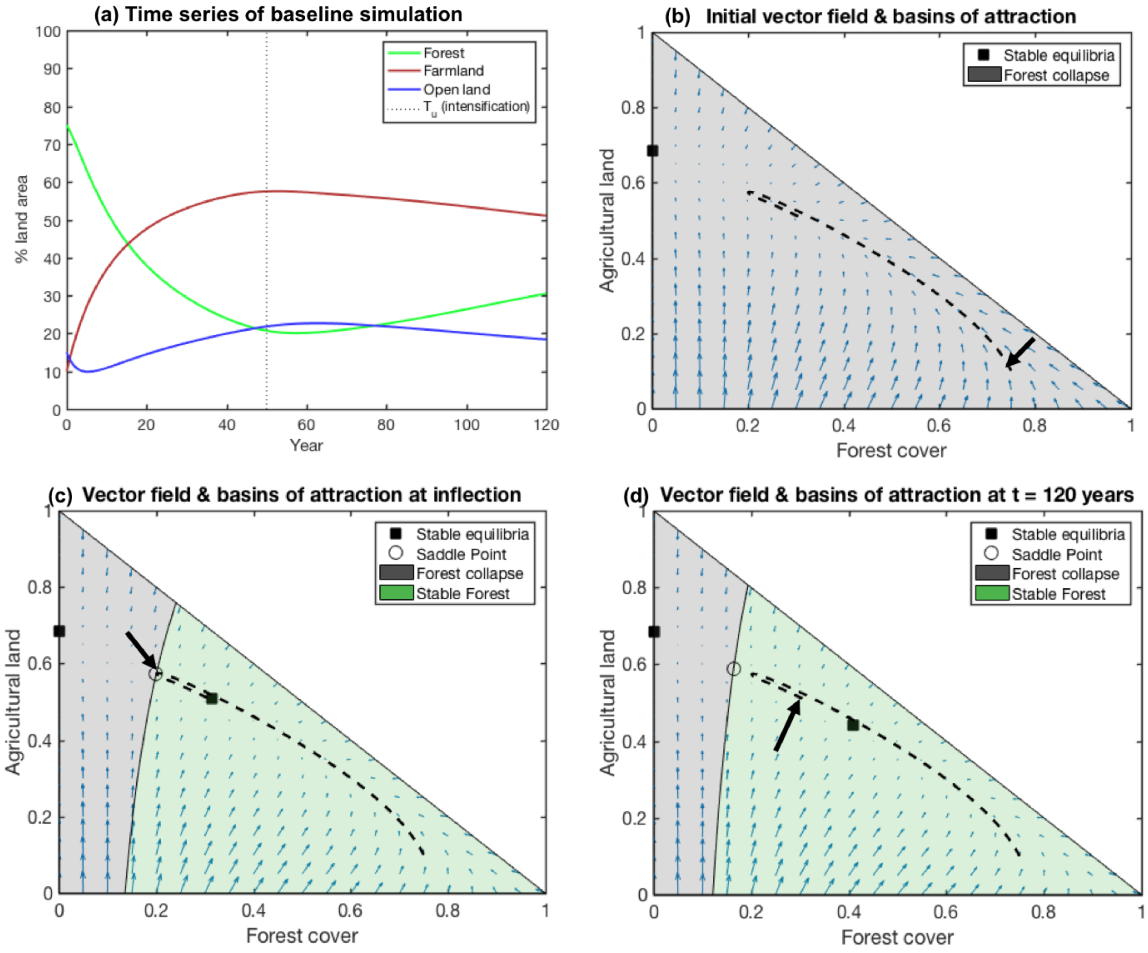

Figure 3.1: In the baseline simulation, forest collapse is narrowly averted by a precisely timed reduction in the forest conversion rate u, leading to a forest transition. (a) Time series of the baseline scenario. The forest conversion rate u decreases smoothly to 40% of its initial value; $T_u = 50$years marks the halfway point of intensification, with u at 70% of its initial value. (b-d) Phase portraits at key times illustrate the time-varying nature of the model. The model is defined within the triangular region $F \geq 0, A \geq 0, A + F \leq 1$, with G as the distance from the diagonal. As intensification occurs, a new interior equilibrium appears due to a bifurcation; the equilibria, vector field, and basins of attraction likewise change. Parameters are $a = 0$, $b = 2$, $h = 15$, $p = 3$, $r = 27$, $\gamma_0 = \gamma_1 = 6$, $u_0 = 4.5$, $u_1 = 1.8$, $v_0 = v_1 = 13$

.

Setting $\dot{F} = 0$ to obtain the equilibria and factoring out F, we find either

$$\begin{cases} \bar{F} = 0 \\ w(\bar{F})(1 - \bar{F}) - b = 0 \end{cases}$$

For the second case, we substitute the definition of $w(F)$:

$$\left(a + r\frac{F^p}{h^p + F^p}\right)(1 - F) = b$$

With $p = 3$, this is a quartic equation with no straightforward solution. However, one root can be approximated by noting that as $F > h$, $F^3 \gg h^3$, so $\frac{F^p}{h^p+F^p} \approx 1$. Then

$$\bar{F} \approx 1 - \frac{b}{a + r}$$

This is the high forest cover state in the absence of agriculture, which is empirically around 80-90% in both tropical and boreal forests [21, 29]. At baseline parameters, there are no other equilibria, and this high forest cover equilibrium is stable, while $\bar{F} = 0$ is unstable. However, changing parameter values can lead to new equilibria and/or change the stability of these equilibria, reflecting different vegetation regimes.

3.1.2 Equilibria with agriculture

To incorporate agriculture, we reintroduce the equation for A:

$$\begin{aligned} \dot{F} = &\quad w(F)F(1 - F - A) - bF - uF \\ \dot{A} = &\quad uF + v(1 - F - A) - \gamma A \end{aligned}$$

Setting the left hand sides to 0, the second equation allows us to solve for $\bar{A}$ in terms of $\bar{F}$:

$$0 = uF + v(1 - F - A) - \gamma A$$

This can be substituted into the F equation derived above, though in general (as previously) a solution can only be found by computer solvers. Within the ecologically relevant domain, the model has 1 or 3 equilibria (Fig. 3.1). In much of the parameter space, the system is bistable, with 3 equilibria: 2 stable nodes and one saddle point. One stable node, corresponding to forest collapse, is at $(\bar{F}_1, \bar{A}_1) = (0, \bar{A}_1)$, while the stable node indicating

forest persistence is at $(\bar{F}_3, \bar{A}_3) = (0, \bar{A}_3)$, with $\bar{F}_3 \cong 40\%$ and $\bar{A}_1 > \bar{A}_3$. The third equilibrium is a saddle node $(\bar{F}_2, \bar{A}_2)$ that lies approximately halfway between the two stable nodes. It is possible to find the equilibria analytically, but only as the roots of a quartic polynomial, so doing so offers little insight and we present a graphical solution instead.

For some parameter values, the system loses bistability. This occurs through a fold bifurcation when the saddle point annihilates one of the stable nodes. Under high conversion rates, such as at $t = 0$ in our baseline simulation (Section 3.4), it is the interior stable state $(\bar{F}_3, \bar{A}_3)$ that is annihilated, so all initial outcomes lead to forest collapse (Fig. 3.1b). However, if conversion rates are low and the low-density forest growth rate a is high, $(\bar{F}_1, \bar{A}_1)$ will be annihilated, and all initial conditions lead to forest persistence.

Under highly specific parameter values, additional interior equilibria appear (Appendix). The conditions required for this to occur are uncommon, and are never reached by altering only single parameter values from the baseline, as the bifurcation diagrams in this chapter indicate. (In principle, since F factors out of the algebraic expression for $\bar{F}$, the equilibria occur as solutions of a polynomial of degree $p + 1 = 4$. The discriminant of this quartic will determine the number of equilibria. However, the discriminant of a quartic equation is a degree 6 polynomial with 16 terms, and the coefficients of the quartic are themselves compound functions of our model parameters; there is the additional step of determining whether any such solutions lie within the ecologically valid region.) Most importantly, the bulk of this thesis focuses on the bifurcation between stability and collapse, and for this research question the distinction between 1 and 2 stable equilibria is of little importance.

3.2 Bifurcation diagrams

The most distinctive feature of this model are bifurcations. Bifurcation diagrams offer a comprehensive and intuitive way to see how these bifurcations occur in each of the model parameters. This offers a clear visual understanding of the effect of model parameters (much more than we can gain algebraically or with intuition).

Diagrams were constructed for both tropical and boreal parameters; since the underlying model is identical, they have identical dynamical behaviour, although they are quantitatively different.

These bifurcation diagrams demonstrate that, under our model, forests are prone to catastrophic collapses. This is expected from introducing ecological thresholds into forest transition modeling, but the bifurcation diagrams provide additional levels of detail. We can see that forests are considerably more sensitive – both in terms of the stable forest

cover, and tolerance to parameter changes before collapse – to agriculturally-determined human parameters (Figures 3.7-3.9) than they are to "natural parameters" only affecting forest growth (Figures 3.2-3.6). While forest collapse can occur due to shifts in natural parameters (e.g. severe drought [20]), it is much more likely to occur as a result of human actions [30], or from a combination of factors [23]. These 1-D bifurcation diagrams only allow us to investigate the effects of single-parameter shifts; however, shifts in multiple parameters tend to have the effects one might expect as a result of combining the effects of the single-parameter shifts (Sections 3.4, 4.3, Appendix).

Strikingly, the forest cover at which collapse occurs is in the narrow range of 20-25% for most parameters. This is somewhat above the value of $h = 15\%$, which we refer to as the threshold for high-density growth. However, due to the functional form used, this is more accurately a half-saturation value (as in Figure 2.2, so 5-10% above this value is a reasonable estimate of where the growth rate begins to decline significantly from its maximal value. The fact that collapses from many possible sources (i.e. changes in b, r, γ, u, v) all occur at nearly the same forest cover suggests that, unlike many other situations [24], the value of the state variable (forest cover) might be of some use as a predictor of collapse risk. Unlike forest cover, the agricultural land cover at the point of this collapse is highly variable (Figures 3.3-3.9). Agricultural land generally increases after forest collapse, but not if the forest conversion rate was higher than the open land conversion rate (Figure 3.8b).

This value for collapse risk aligns fairly well with Environment Canada's recommended guideline of minimum forest cover. This states "30% forest cover at the watershed scale is the minimum forest cover threshold. This equates to a high-risk approach that may only support less than one half of the potential species richness, and marginally healthy aquatic systems [45]." This metric was devised largely based on the requirements for bird habitat, but cautions that true thresholds are site- and species-dependent and often unknown. In our model, this corresponds to uncertainty in the value of h.

3.2.1 Bifurcations in natural parameters

In this section we consider the impact of natural parameters. As stated previously, these are intrinsic to the forest dynamics. They may change slowly, in particular due to climate change or varying moisture levels. They may also be affected by human action, which could be through direct means such as tree planting (for the low-density growth rate a) or by indirect means such as spreading invasive species or otherwise altering the ecology of the community.

While we want to understand how the model responds to these changes, we are much

more concerned about synergies between changes in natural parameters with changes in human parameters that we are with changes in natural parameters in isolation [23].

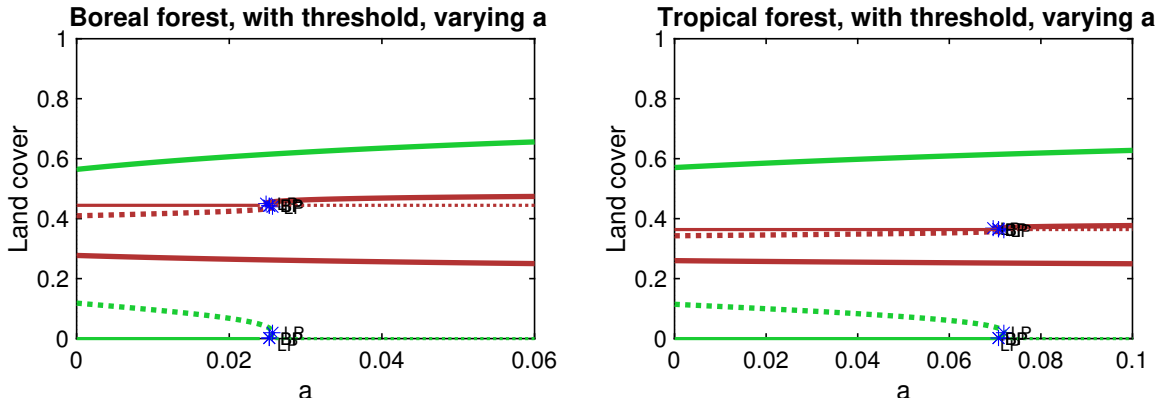

Figure 3.2: Bifurcations in a, the low-density forest growth rate, for (a) boreal forest and (b) tropical forest. Green and red lines correspond to equilibrium forest and farmland cover, respectively. Solid lines represent stable equilibria, and dashed lines represent saddle points. The thick lines indicate the interior equilibrium, and the thin lines indicate the $F = 0$ equilibrium. "LP" stands for "Limit Point", indicating the cusp bifurcation.

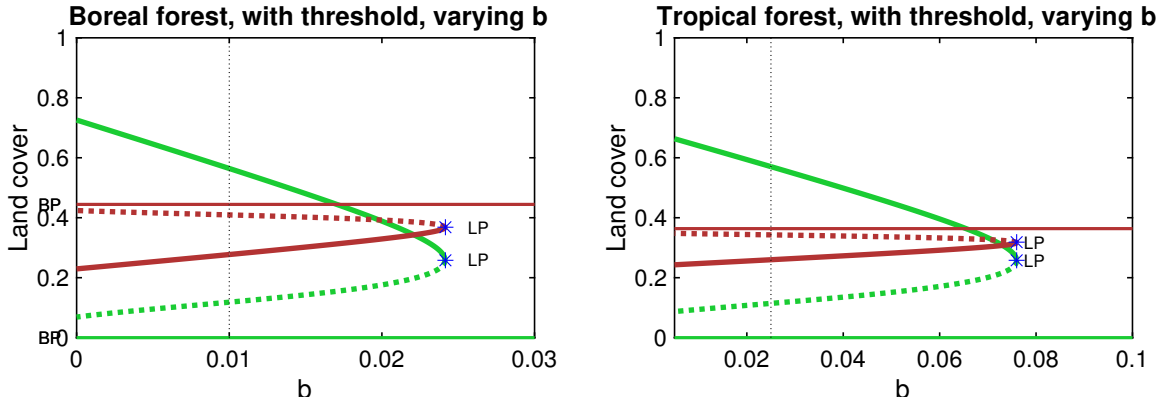

Figure 3.3: Bifurcations in b, the natural forest disturbance rate, for (a) boreal forest and (b) tropical forest. Green and red lines correspond to equilibrium forest and farmland cover, respectively. Solid lines represent stable equilibria, and dashed lines represent saddle points. The thick lines indicate the interior equilibrium, and the thin lines indicate the $F = 0$ equilibrium. "LP" stands for "Limit Point", indicating the cusp bifurcation.

When a is low, the $F = 0$ equilibrium corresponding to forest collapse is stable (Fig. 3.2). As a increases, this equilibrium loses stability – this is a transcritical bifurcation

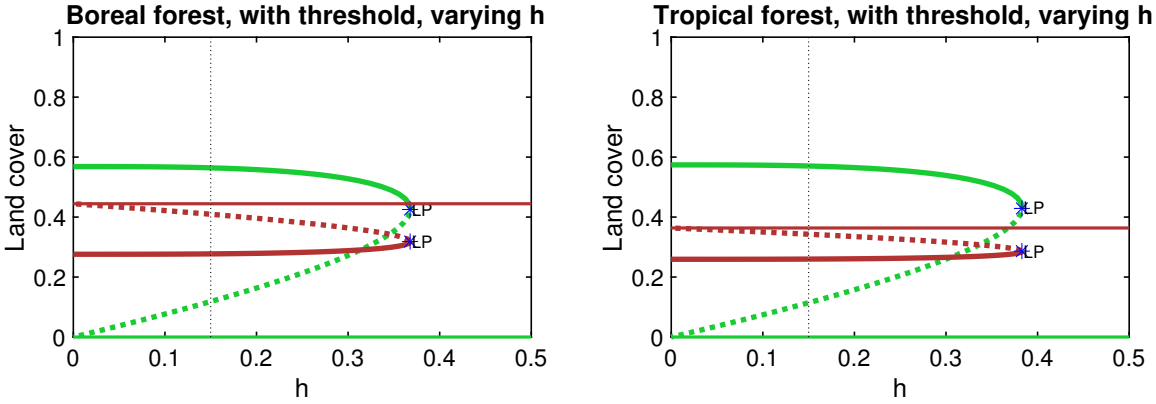

Figure 3.4: Bifurcations in h, the half-saturation value of the Hill function for density-induced feedback in forest growth, for (a) boreal forest and (b) tropical forest. Green and red lines correspond to equilibrium forest and farmland cover, respectively. Solid lines represent stable equilibria, and dashed lines represent saddle points. The thick lines indicate the interior equilibrium, and the thin lines indicate the $F = 0$ equilibrium. "LP" stands for "Limit Point", indicating the cusp bifurcation.

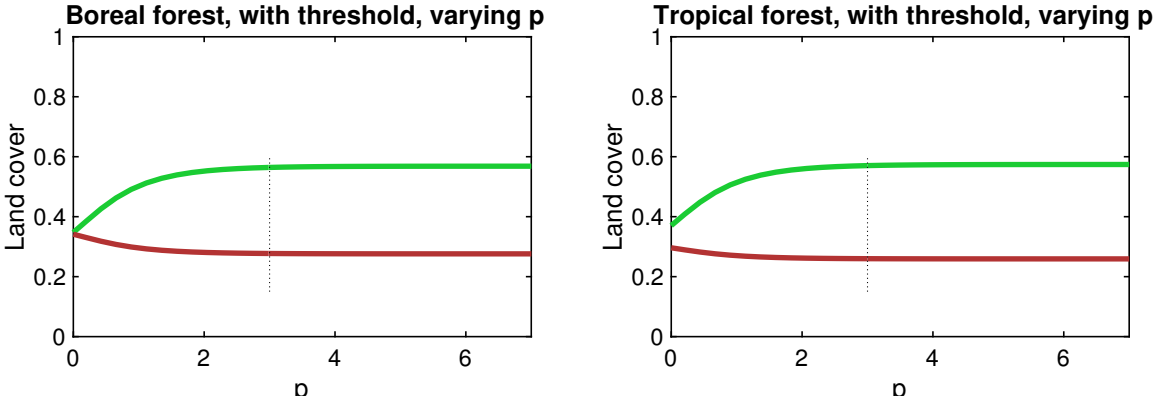

Figure 3.5: Bifurcations in p, the steepness parameter for density-dependent forest growth, for (a) boreal forest and (b) tropical forest. Green and red lines correspond to equilibrium forest and farmland cover, respectively. Solid lines represent stable equilibria, and dashed lines represent saddle points. The thick lines indicate the interior equilibrium, and the thin lines indicate the $F = 0$ equilibrium. "LP" stands for "Limit Point", indicating the cusp bifurcation. Sensitivity to p is negligible, so it was kept fixed at $p = 3$ for all subsequent analysis.

leading to monostability of the interior equilibrium. The interior equilibrium value also

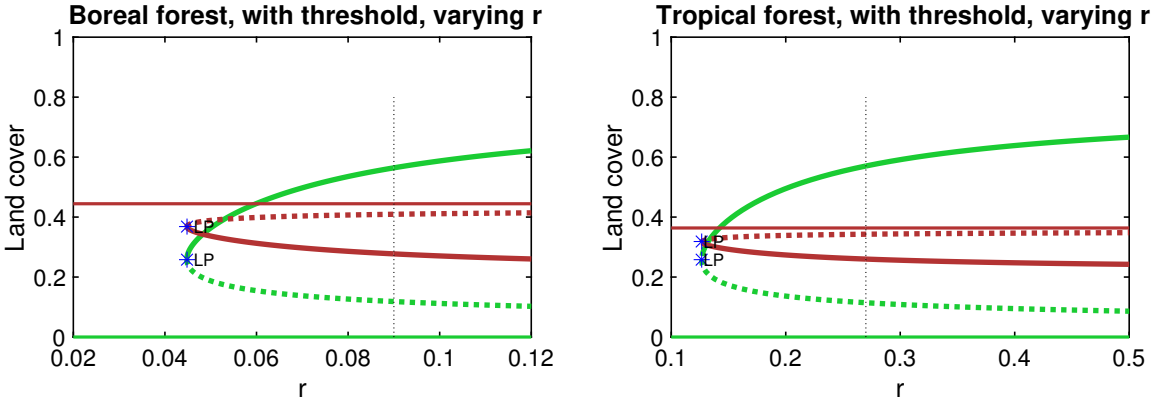

Figure 3.6: Bifurcations in r, the increase in growth rate for high-density forests, for (a) boreal forest and (b) tropical forest. Green and red lines correspond to equilibrium forest and farmland cover, respectively. Solid lines represent stable equilibria, and dashed lines represent saddle points. The thick lines indicate the interior equilibrium, and the thin lines indicate the $F = 0$ equilibrium. "LP" stands for "Limit Point", indicating the cusp bifurcation.

increases slightly as a increases, but changes in a do not change its stability.

The natural disturbance rate is likely to increase with climate change and drought. Changes in b have a moderate impact on the location of the internal steady state, but do not impact the stability of the system except for very extreme values, which induce a bifurcation to forest collapse (Fig. 3.3).

Changes in h, the half-saturation value for forest growth, affect the value of the unstable saddle, and consequently the basin boundary between stable forest and collapse (Fig. 3.4). As h becomes very large, this saddle point collides with the interior equilibrium, in a fold bifurcation leading to forest collapse. Prior to this point, changes in h have almost no effect on the location of the interior equilibrium, and unless cover levels are low it is difficult to accurately parameterize h.

The steepness parameter p has almost no effect on the dynamics (Fig. 3.5). The numerics did not converge for the saddle point in this case. However, there is almost no effect of p on the interior equilibrium, and within the viable range there are no bifurcations. Due to this very low sensitivity we have fixed $p = 3$ throughout this work, to reduce the dimensionality of parameter space.

Changes in r have a substantial impact on the location of the interior equilibrium, and little impact on the unstable equilibrium (Fig. 3.6). Extremely low values will induce a

bifurcation to forest collapse. This parameter can be estimated fairly accurately based on growth data, and is likely to be influenced by climate change, e.g. increasing in Quebec boreal forests due to rising temperature and precipitation [40].

3.2.2 Bifurcations in human parameters

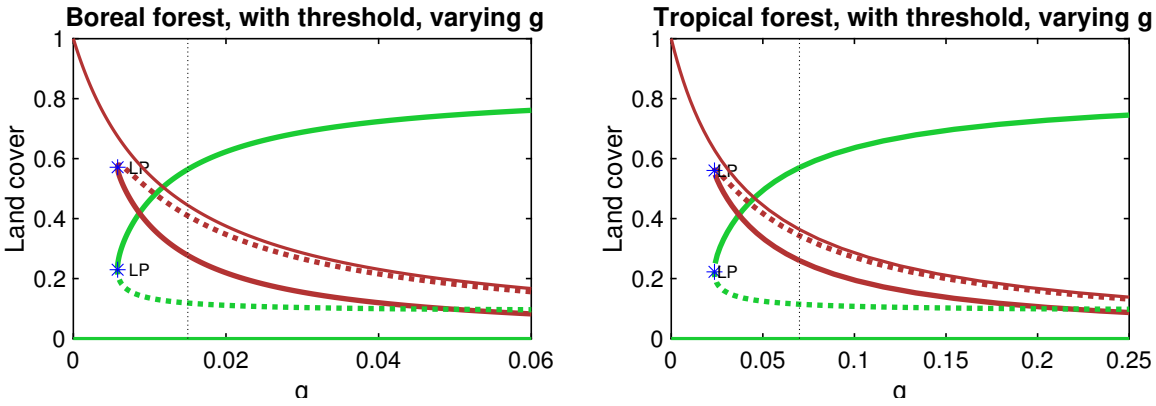

Figure 3.7: Bifurcations in γ, the agricultural abandonment rate, for (a) boreal forest and (b) tropical forest. Green and red lines correspond to equilibrium forest and farmland cover, respectively. Solid lines represent stable equilibria, and dashed lines represent saddle points. The thick lines indicate the interior equilibrium, and the thin lines indicate the $F = 0$ equilibrium. "LP" stands for "Limit Point", indicating the cusp bifurcation.

As the farmland abandonment rate decreases ($\gamma \to 0$), the agricultural area markedly increases with a corresponding decrease in forest cover, until a bifurcation occurs (Fig. 3.7). At this bifurcation, forest cover collapses to 0, and agricultural cover increases slightly. The sensitivity to γ is very large.

Changes in the forest conversion rate u have a large effect on the location of the interior equilibrium, and increases soon lead to forest collapse (Fig. 3.8). If $u > v$ at the point of collapse, as in the tropical case shown here, agricultural land will *decrease*, as open land is being farmed less aggressively than the now-extirpated forest. Sensitivity to u is also large.

Changes in the open land conversion rate v have a similar effect, although less dramatically (Figure 3.9). Though forest is not being cleared directly, increases in v still lead to reduction in forest cover and then collapse, since to maintain its size the forest requires readily available open land. Relative sensitivity, as can be seen from the steepness of the

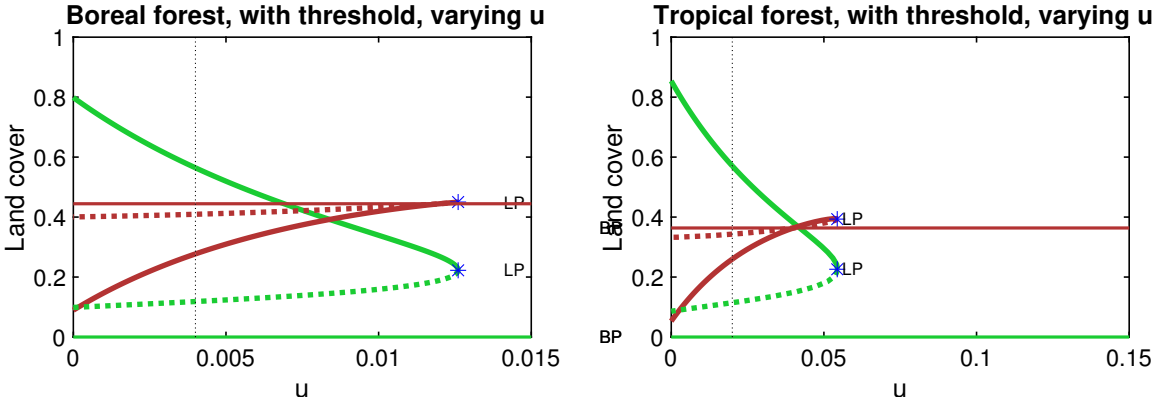

Figure 3.8: Bifurcations in u, the forest conversion rate, for (a) boreal forest and (b) tropical forest. Green and red lines correspond to equilibrium forest and farmland cover, respectively. Solid lines represent stable equilibria, and dashed lines represent saddle points. The thick lines indicate the interior equilibrium, and the thin lines indicate the $F = 0$ equilibrium. "LP" stands for "Limit Point", indicating the cusp bifurcation.

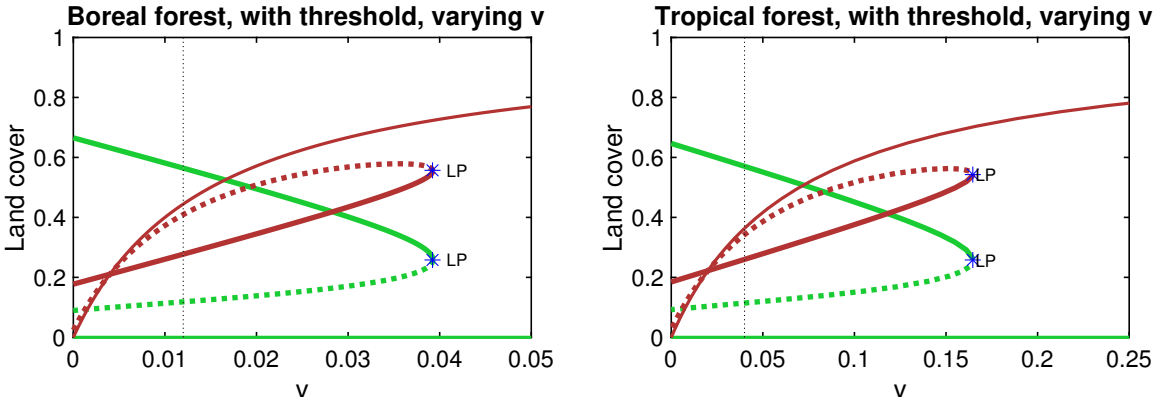

Figure 3.9: Bifurcations in v, the open land conversion rate, for (a) boreal forest and (b) tropical forest. Green and red lines correspond to equilibrium forest and farmland cover, respectively. Solid lines represent stable equilibria, and dashed lines represent saddle points. The thick lines indicate the interior equilibrium, and the thin lines indicate the $F = 0$ equilibrium. "LP" stands for "Limit Point", indicating the cusp bifurcation.

curve on the bifurcation diagram, is of similar magnitude for v as for u, though the absolute sensitivity is much smaller, since the range of v is quite broad.

3.3 Metrics of resilience and recovery

3.3.1 Metrics of ecological resilience

While resilience is a topic of primary interest to mathematical ecology, and the broader field has various methods to quantify resilience, these have less often been applied in the sub-field of forest transition scholarship. These measures, such as distance from undesirable tipping points or the distinct but related concept of being able to withstand small perturbations, are often used in models of coupled human-environment systems [46]. However, much of the associated theory, such as early warning signals for critical transitions, is based on equilibrium analysis of the system. This means that it does not apply in our case, where slow dynamics of forest cover (i.e. on the order of decades, even if parameter changes are faster) ensure very long transients. Given these limitations, we apply two more fundamental definitions of resilience, as described by Walker and colleagues [47]. Of the four aspects of resilience they identify, we apply two: precariousness and resistance. Precariousness measures how close the system is to a threshold; for our system, we define it as the distance in phase space between the point of minimum forest cover and the basin of attraction for forest collapse. It also represents the largest perturbation the system is guaranteed to withstand. Resistance, by contrast, represents the ease or difficulty of changing the system. This can be determined by how quickly the the system returns to equilibrium after a perturbation, which is controlled by the dominant (i.e. largest in magnitude) eigenvalue at the stable forest equilibrium. This is indicated by λ (Figure 3.12), with more strongly negative values of λ indicating greater stability. Although eigenvalues of a particular equilibrium are a purely local phenomenon, they can often convey more information about system behaviour [25].

3.3.2 Metrics for recovery

In addition, we define a pair of measures for the extent of forest recovery following a potential forest transition. The first is a qualitative hierarchy based on the overall trajectory of the time series (Figure 3.10), which was first defined by Pagnutti *et al.* [4]. We frame it here as a metric of recovery, following the definition of adaptability as "changing the current state of the system so as to move either deeper into a desirable basin, or closer to the edge of an undesirable one" [47]. The second measure is simply the increase in forest area a specified time after the transition. This is quantitative and more straightforward, but arbitrary in certain ways that limit its applicability. Note that our measures of forest recovery are entirely distinct from restoration, which consists of achieving an ecological transition

from the steady state of forest collapse to forest persistence [48], which we consider outside the scope of the present work.

3.4 Simulations

3.4.1 Model for agricultural intensification

To reflect agricultural intensification (i.e. a change in land use patterns whereby agriculture is concentrated in productive lands, allowing marginal lands revert to a natural state), model parameters for agriculture must change over time. These changes occur to the parameters $\{\gamma, u, v\}$ that describe conversion to and from agricultural land.

We capture this change with a sigmoidal function varying smoothly from the initial value to a final value. This sigmoid is parameterized by the time of the transition (the midpoint between final and initial values) and by a steepness term, governing the time scale of the transition. For the forest conversion rate $u(t)$, the initial and final value are u_0 and u_1, and the parameters for transition time and timescale are, respectively, T_u and k_u. The exponential sigmoid is given by

$$u(t) = u_0 + (u_1 - u_0)\frac{1}{1 + \exp\left(k_u(T_u - t)\right)} \tag{3.2}$$

The graph of $u(t)$ is illustrated in Figure 3.11; functional forms for $\gamma(t)$ and $v(t)$ were identical. This makes the system of DEs inhomogeneous. The timescale of parameter change and of system dynamics are both on the order of decades.

For the land conversion parameters $\{\gamma, u, v\}$, both the initial and final values lay within the ranges on Table 2.1. The timing parameters T_i and k_i were chosen to represent realistic forest transitions, with land use intensification occurring near the midpoint of each simulation, and the transition between land use regimes taking approximately 5-20 years.

Note that, although intensification typically entails abandonment of farmland (especially marginal lands) [35, 11], the annual rate of farmland abandonment γ will often decrease with intensification. This counter-intuitive parameter shift is based on several contributing factors. Firstly, the remaining high-quality land will have less turnover. Secondly, decreasing conversion rates ensure that net agricultural area will still decrease. Thirdly, the decrease in farmland abandonment typically occurs after the decrease in the conversion rates (i.e. $T_\gamma > T_u, T_v$). This is because the cost to clear and plant new cropland

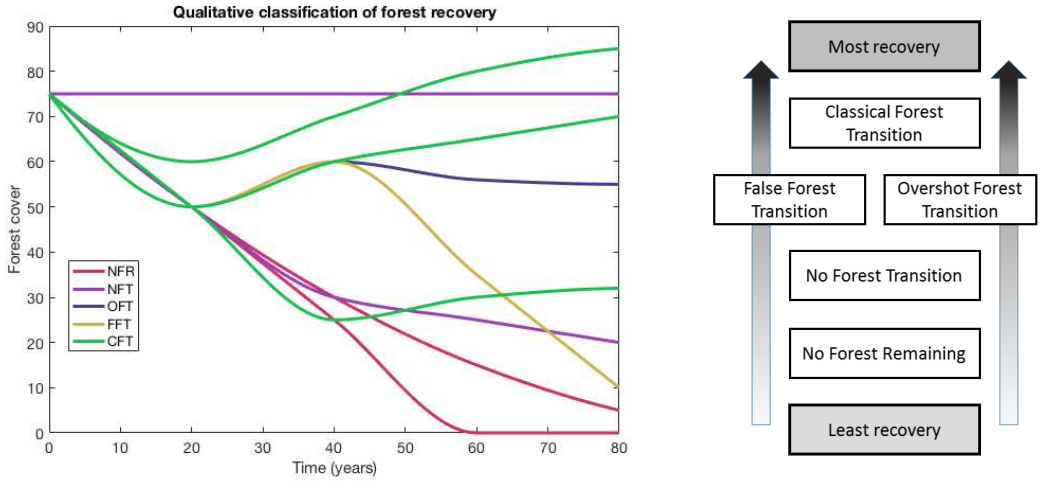

Figure 3.10: Qualitative classification of recovery outcomes, based on the extrema of forest cover, from [4].

- No Forest Remaining: Final forest below a cutoff level of 10%
- No Forest Transition: No local minimum; can be either no decline, or a steady decline with more than 10% forest cover remaining at the end of the time series
- Overshot Forest Transition: Global minimum followed by local maximum
- False Forest Transition: Local minimum followed by local maximum and subsequent decline
- Classical Forest Transition: Global minimum only

Simulations that fall into the same qualitative classification may have very different final forest cover levels, as illustrated. Subsequently in this work, Overshot Forest Transition and False Forest Transition are grouped into a single category, since both are very uncommon.

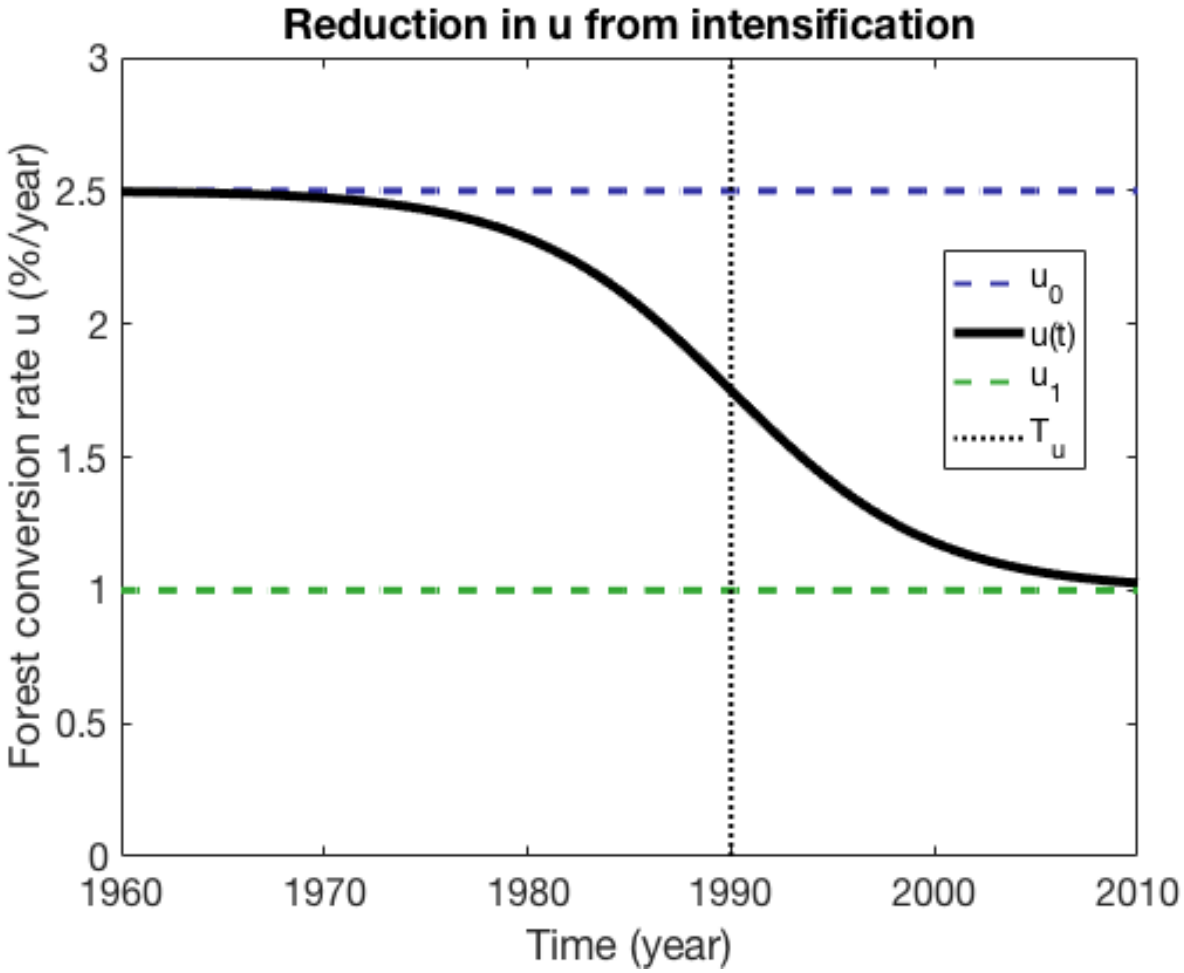

Figure 3.11: Time-varying forest conversion rate $u(t)$, as land use intensification reduces the forest conversion rate. The time of intensification $T_u = 1990$ marks the midpoint between the initial high forest conversion and subsequent low forest conversion; the timescale of the change is given by k_u.

is generally greater than the maintenance cost of existing farmland. The net abandonment of agricultural land occurs during this period when the annual abandonment rate outstrips the annual conversion rates.

3.4.2 Simulation setup

For both tropical and boreal parameter values, we generate a baseline transition scenario. This was chosen to exemplify a forest transition that comes as near to collapse as possible, so that it i) shows a prototypical example of a forest transition (while lying well within the established parameter ranges) and ii) allows small perturbations in parameter values to tip the balance between recovery and collapse.

The goal of these simulations was to determine the impact of human-influenced parameters – both the initial values and the changes at the time of agricultural intensification – on system output. An ensemble of 100,000 parameter sets was generated from perturbations of agricultural parameters from the baseline simulation (Figure 3.1) and used to simulate the differential equation system, from the same initial condition $(F, A) = (0.75, 0.1)$ as in the baseline scenario. One set of simulations was conducted with all parameters varying, and one set was conducted with the natural parameters $\{a, b, h, r\}$ held fixed at the values specified in the baseline scenario, to isolate the effects of the human-controlled parameters. Simulations were conducted for both tropical and boreal scenarios.

All simulation runs were ordinary differential equations, implemented in MATLAB using `ode45`. The only source of randomness was the selection of parameters; the simulation was deterministic. Each realization of the randomly generated parameters was passed to the ODE function. After specifying the initial condition and time span (all of which were identical to the baseline simulation), the output was analyzed for local stability properties, local extrema, and other properties required to compute the metrics of resilience and recovery described above. Local extrema that only dominated surrounding points by a small amount (1% cover) were rejected to eliminate computational artefacts, and because even a true forest transition The distance to collapse was analyzed by first analytically identifying the saddle point and separatix (via an inverse time trajectory beginning along the appropriate eigenvector), and then computing the minimum distance to the solution curve.

MATLAB code implementing the above calculations, including a list of scripts to generate each figure, are found at the repository given in the appendix.

3.4.3 Results

Our analysis has shown that forest collapse can occur in situations where agriculture and ecological thresholds occur together (Figures 3.2-3.9). Simulations show that trends of resilience measures (minimum distance from collapse and resistivity to perturbations) and

recovery measures (inflection points in forest cover and total regrowth area) follow broadly similar patterns as the risk of collapse (Figures 3.12, 3.13). Parameters associated with agriculture have a larger impact on the risk of forest collapse than natural forest parameters. The most important parameter for determining the risk of collapse is the initial farmland abandonment rate γ_0. This has a clear threshold effect, in that if γ is sufficiently large the risk of collapse is negligible. Agricultural conversion rates u (forest conversion) and v (open land conversion) also have a considerable effect. Changes at the time of land use intensification have very little impact on resilience, and only have small effect on forest recovery.

Results were very similar for tropical and boreal parameters, as shown in the bifurcation diagrams. For applicability and policy considerations, we are most interested in the ensemble simulations of tropical forests. The reasons are twofold: (a) fewer tropical countries have so far undergone a forest transition, so interventions to increase forest resilience are more necessary, and (b) the shorter time scale decreases the chance of unforeseen external factors invalidating the model.

The most important parameter for determining the risk of collapse is the initial farmland abandonment rate. For $\gamma_0 \approx 0$, the chance of collapse is almost 100% (Figure 3.12). As agricultural abandonment increases, the risk of collapse declines rapidly, to less than 10% for γ_0 of 12% annually. Beyond the regime where collapse is very unlikely, further increases in γ_0 continue to increase the system resilience, as measured by distance from threshold. Resistivity displays similar dependency on this parameter. Conversely, the two recovery metrics display much less sensitivity to further increases in γ_0 (Figure 3.13). In contrast to the strong effect of γ_0 on collapse risk, reduction in γ at the time of intensification has a very weak effect on collapse risk and on resilience. It does impact recovery – reducing γ_1 can turn a very resilient Classical Forest Transition into a much less resilient False or Overshot Forest Transition, and can similarly increase the extent of forest regrowth – but these beneficial outcomes are only seen in a relatively small minority of cases.

The forest conversion rate u_0 and the open land conversion rate v_0 have a similar degree of impact on the risk of collapse. Unlike with γ_0, their impact is linear across the entire range of the parameter, from almost no chance of collapse for u_0 and v_0 near 0, to 60% risk at the upper limit of each parameter. In spite of this similarity, the impact of u_0 is much more severe, since its range is much smaller; furthermore, when collapse is avoided, it has a much larger impact on both metrics of resilience. The forest conversion rate is also the best target to reduce at the time of intensification: doing so can reduce the risk of collapse from around 45% to 25%. As with γ, reducing the conversion rates has little impact on the distance from threshold, but a substantial impact on the qualitative resilience metric. Even where collapse is avoided, these reductions will often move the system from No Forest

Transition to Classical Forest Transition, going up two levels on the hierarchy.

These results show that the gradual encroachment of farmland (and hence lack of available room to expand) is at least as severe a threat to forest as direct land conversion. After intensification, increasing γ and decreasing u remain important in optimizing resilience by the qualitative metric. However, the gains in resilience are quite marginal if we are measuring distance from collapse. This is because most of the impact of intensification occurs after the inflection point, so the timing or location of this point does not change.

This difference in effect of the initial and intensified parameters occurs because the resilience measures are entirely determined at the point of transition, which in turn depends on the initial forest loss. The intensified parameters only change system properties after this inflection point has occurred (or to a very small extent as it is about to occur); this is precisely the time window that is reflected in the metrics of forest recovery.

Comparing all four metrics, we find that distance from collapse has the best discrimination, in that it splits the ensemble space more evenly than any of the other three metrics. For example, at some parameter values (such as high u_0), the intermediate levels of the qualitative recovery hierarchy do not occur, so this metric offers little more than a binary classification between collapse or forest persistence.

Somewhat surprisingly, considering the strong similarity in their responses to parameter changes, we find that the relationships between each of our metrics of resilience and recovery are quite weak (Figures A.2-A.4; no scatter plots were produced for the qualitative recovery metric)). This suggests that it is worth collecting information on each of these measures and that none is redundant, even if they may all suggest the same choices of parameters (i.e. high γ, low u and v) to ensure robust forest cover.

We also considered cross-effects of multiple parameters on resilience, as measured by distance from collapse (Figures A.5-A.7). The cross-effects between the key parameters γ_0, u, v are prominent and as expected, in that collapse risk is higher if two parameters simultaneously change in directions that would increase it, and so on. Cross-effects between any other parameters are quite weak. Surprisingly, this includes the timing parameters T_γ, T_u, T_v (Figures A.8 - A.10); interactions between the base parameter and its associated timing parameter (within the distribution we selected) seem to have no strong effect on system resilience. This further emphasizes the importance of the initial parameters as compared to any changes at the time of intensification.

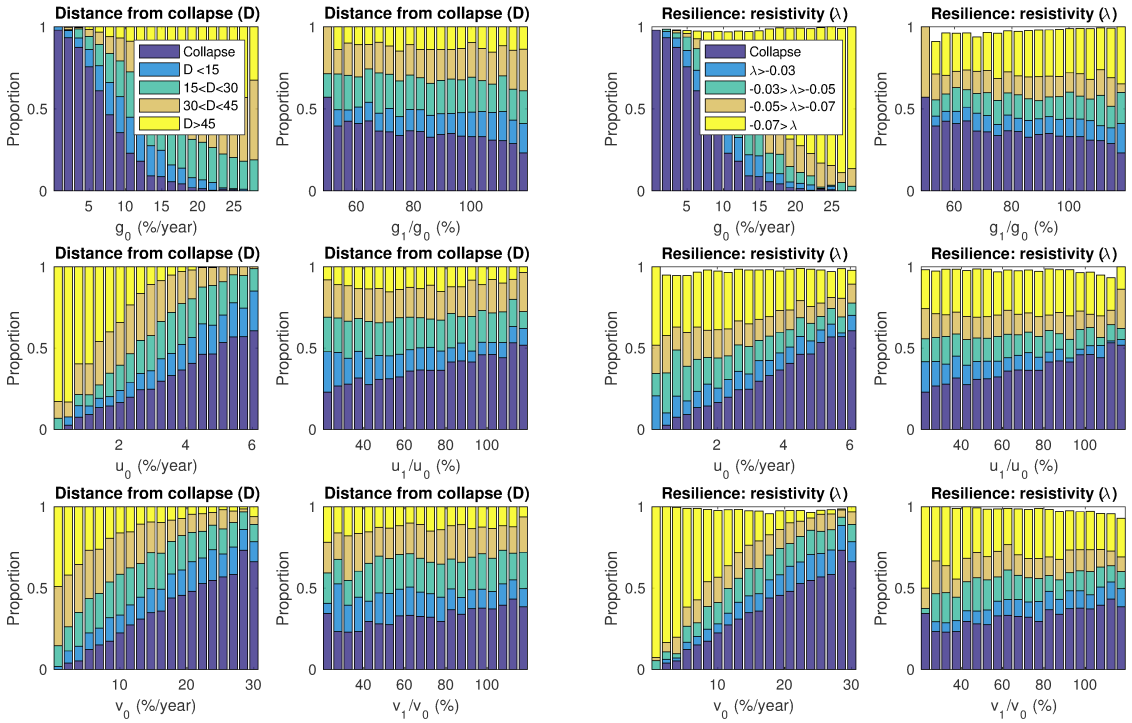

Figure 3.12: Two measures of forest resilience. Columns 1 and 2 shows how the latitude, or minimum distance from collapse (D), depends on the initial parameters (Column 1) and on changes at the time of intensification (Column 2). Columns 3 and 4 show how the resistivity, as measured by the magnitude of the dominant eigenvalue at the stable forest equilibrium, depends on initial parameters (Column 3) and on changes at intensification (Column 4).

Both resilience metrics show very similar results, indicating that either one is a good measure of resilience in this system. The most significant patterns in this data are driven by simulations with forest collapse (the distribution of collapses is by definition identical across both metrics). We see that the initial parameters have pronounced effects on collapse, while land use intensification makes very little difference. The distribution of intermediate resilience states follows similar patterns to the distribution of collapses. For both metrics, γ has the strongest effect, with 100% collapse as $\gamma \to 0$ and a threshold of $\gamma \approxeq 15$ above which persistence is almost guaranteed. The land conversion rates u and v have weaker but still substantial effects, from 0% collapse risk to 60% at the maximal value of each parameter. However, sensitivity to forest conversion u is much higher, since its range is smaller.

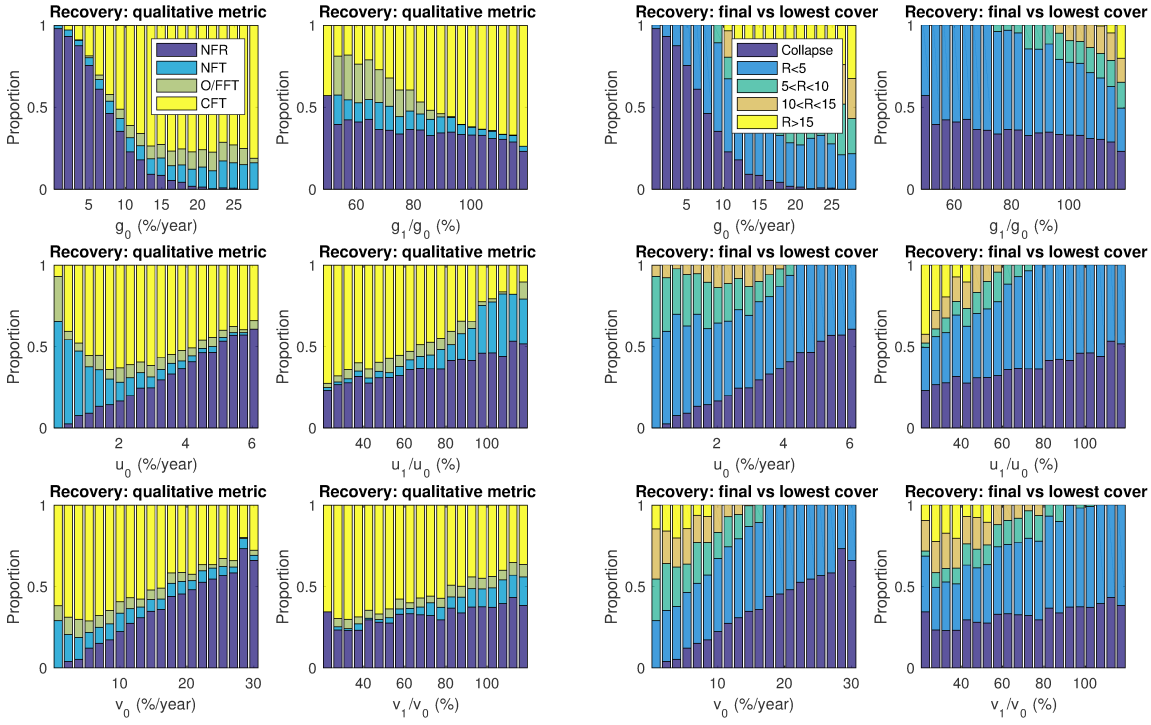

Figure 3.13: Metrics of forest recovery. Columns 1 and 2 shows how the qualitative characterization of forest recovery depends on the initial parameters (Column 1) and on changes at the time of intensification (Column 2). Columns 3 and 4 show how the absolute gain in forest cover depends on initial parameters (Column 3) and changes at intensification (Column 4).

As with the resilience measures, the initial parameter values still largely determine whether or not collapse occurs, and collapse precludes forest recovery. However, unlike the resilience measures, changes in parameter values at the time of intensification have a considerable effect. In particular, lack of reduction in u, or a large decrease in γ, often means that even if the forest has avoided total collapse it remains in decline.

Chapter 4

Real-world data and predicting collapse risk

In this chapter, we describe two different adaptations of the model to fit real-world data. In the first adaptation, the parameters are continuous functions of time, following the land use intensification model of Section 3.4. This first adaptation is a post-hoc analysis, allowing us to see the factors influencing empirical forest transitions. In the second adaptation, the parameters are discrete functions of time, calibrated every five years as new data becomes available. This is more predictive, as it allows us to extrapolate future land cover based on current trends; it incorporates an ensemble approach as a means to address uncertainty. This addresses a major limitation of the previous chapter, which was that collapse could only be predicted in the unrealistic situation of known parameter values.

4.1 Data

We obtain historical land cover data for three countries – China, Costa Rica, and Vietnam – from Lambin and Meyfroidt (2011) [10]. These countries were selected because they underwent forest transitions in the second half of the 20th century, and they have good data available over an extended period. Data on agricultural land at the national level since 1960 can be reliably found from the United Nations Food and Agriculture Organization's FAOSTAT database [49], but until recent decades when satellite imaging became prominent, reliable data on forest cover was scarce. Since the timescale of interest for forest transitions is decades at a minimum, the present work relies on Lambin and Meyfroidt's

interpolated data for forest cover values [10]. An error in their record of agricultural land in Costa Rica post-1985 was fixed with reference to FAO data [49].

4.2 Continuously varying parameters

For the continuous time model, we are interested in obtaining the best fit of the land use intensification model described in Section 3.4. There are a total of sixteen parameters to fit. Four come from the constant natural parameters a, b, h, r (p is assumed fixed at 3, due to very low sensitivity), and twelve from the varying agricultural parameters. For each of u, v, γ, there is an initial value, a final value, a time of transition, and a steepness of the transition. We assume that two values of each agricultural parameter are sufficient, since most of the forest transition literature speaks in terms of a shift between two regimes [12].

The fitting method to determine these parameters is bounded simulated annealing, as implemented in the MATLAB function `@simannealbnd` A sample run is shown in Figure 4.1a. Simulated annealing is an iterative algorithm for approximating global optima in large search spaces; the use of an internal "temperature" variable to control the probability of moving away from a local minimum simulates an analogous process in metallurgical annealing, hence the name. The steps of the algorithm are:

1. Let $\beta = \beta_0$ and evaluate the objective function $f(\beta)$ (in this case, model error as described below)
2. Decrease the temperature T
3. Randomly sample (from a multivariate normal distribution, within the specified bounds) a nearby parameter vector β_1
4. Evaluate the objective function (model error) on this input, $f(\beta_1)$
5. If $f(\beta_1) < f(\beta_0)$ (i.e. there is an improvement in the objective function), set $\beta \leftarrow \beta_1$ with high probability. If not, rather than rejecting β_1, set $\beta \leftarrow \beta_1$ with some non-zero probability that is an increasing function of temperature.
6. Repeat these steps until the temperature T reaches a minimum value, or a large number of steps have passed with no significant improvement in β.

There are many options available for the function by which the temperature decreases in Step 2 and the acceptance probabilities in Step 5. The key is that temperature should decrease over time, and the probability of moving out of a local minimum should be high when temperature is high and should be low when temperature is low. Specifics for the use of the `@simannealbnd` function in this project are described in code repository listed in the appendix.

To perform this fit, we require a measure of the error between a parameter set and a data series. We use the simple sum of Euclidean errors. To be more precise, let $\beta = [a, b, h, p, r, \gamma(t), u(t), v(t)]^T$ be a parameter set (noting that γ, u and v are functions of time) and $\mathbf{x} = x_{t,i}, t \in \{t_0, \ldots, t_N\}, i \in \{1, 2\}$ be a data set, indexed by year and by land cover type (forest and agricultural land). To define an error function:

1. Simulate the differential equation solution with the given parameters, using the first data point $(x_{t_0,1}, x_{t_0,2})$ as the initial condition. Evaluate the simulated solution at the same time points as the original data series, and call this simulated solution $\hat{\mathbf{x}}(\beta) = \hat{x}_{t,i}$

2. Define the error as the sum of the Euclidean distances between $\mathbf{x}$ and $\hat{\mathbf{x}}(\beta)$ at each year:

$$\text{Error} = \sum_{t=t_0}^{t_N} \sqrt{(x_{t,1} - \hat{x}_{t,1})^2 + (x_{t,2} - \hat{x}_{t,2})^2} \tag{4.1}$$

   This is the sum over all years of the 2-dimensional (forest and farmland) distances between the data and the model.

Having defined the error function, we only need to set the bounds for each parameter estimate, as well as the initial estimate. The bounds on the parameter space for the algorithmic fitting are taken from the literature as summarized on Table 2.1, with only very slight modifications to ensure reasonable values. The precise values of the simulated annealing parameters are shown on Table 4.1, along with the fitted values. For the simulated annealing metaparameters, the system was initialized with a high initial temperature (1500) and re-annealed frequently to sufficiently explore the 16-dimensional parameter space. For each country, the algorithm completed successfully in less than 20,000 steps by reaching the threshold value for function improvement. A sample run is shown in Figure 4.1a, and information about the code is included in the appendix.

4.2.1 Results and discussion

The model fits broad trends in the data fairly well (Figure 4.1). In all cases, errors are due to the model being smoother than the data. For China, the modelled agricultural land cover continues to rise smoothly, instead of abruptly levelling off in the late 1980s. For Costa Rica, the model is unable to make as steep a decline and recovery as the data. For Vietnam, the model averaged over the forest cover after 1980, instead of tracking the slight decline and subsequent large recovery beginning in the late 1990s. This smoothness of the fitted model is expected behaviour for a differential equation.

These errors, along with the underdeterminacy of the parameters in this system (see below) suggest that we cannot be entirely confident in the fitted parameter values. However, it is still instructive to examine the relative changes characterizing each country's forest transition.

For China, the fitted parameters showed considerable increases in u and v, along with a slight increase in γ. However, the changes in u and v come in the 1960s, which is early enough that the initial values have little effect. And while the change in γ is much smaller in magnitude, Chapter 3 demonstrated the model's high sensitivity to γ, so this may have a moderate effect on forest resilience despite the lack of transition in the fitted model.

For Costa Rica, we see that the changes in u and v are not very significant. The change in u occurs very early, in 1963, and the change in v is negligible in magnitude. For the most part, this pronounced forest transition was driven by an increase in the farmland abandonment rate γ. However, it is instructive to note that the levelling off of agricultural land begins well in advance of T_γ, which is in 1989. The forest's subsequent recovery can be attributed to very high growth parameters a and r.

For Vietnam, the forest conversion rate u plays a surprisingly small role. Both its initial and final values are much smaller than other parameters, and it decreases right at the beginning of the time series, in 1961. Instead, the dynamics of forest change in Vietnam are driven by γ and v. The slight decrease in γ in 1980 corresponds to the slight decrease in the forest loss rate at about the same time, and the 1993 increase in v corresponds to the expansion of agriculture. Unfortunately, the fitted model does not capture the accompanying rise in forest cover, and so does not produce a forest transition. the fitted model also found a very high natural disturbance rate b and low growth rates a and r, suggesting that the forest would have difficulty recovering. The mechanism behind the post-1980 forest transition would be an interesting one to consider, as the simultaneous increase in forest and farmland cover contradicts classical forest transition theory [3]. However, land use is intimately tied to large-scale political issues, and the difficulties of recovering from

the Vietnam war make this an anomalous example. This should not affect the baseline viability of the model, but it does imply that initial open land G was unusually large, such that the classical tradeoff between forest and agriculture did not apply.

While it is both necessary and informative to fit our model to real-world data, this continuous time approach is more limited than we might have hoped. There are several issues: fits are approximate, and even time-varying parameters sometimes fail to capture forest transitions. In addition, these are all post-hoc fits, in that they were based on the entire time series. This is useful for analysis of the factors involved in real-world forest transitions and for establishing model validity, but offers no benefit in anticipating or preventing forest collapse.

4.3 Discretely varying parameters

To complement the continuous time model and address some of its shortcomings, we develop an alternative method for fitting parameters in discrete time. For this method, we divide the data series into overlapping subintervals, and estimate the parameter values on each subinterval.

Instead of estimating a single set of parameter values as we did in the continuous-time model, we estimate an ensemble of parameter values. This is to address the underdetermination of the system and acknowledge uncertainty.

The precise fitting method is:

1. Divide the 50 year time period (1961-2010) into 8 overlapping subintervals of 15 years each: [1961-1975], [1966-1980], ..., [1996-2010]

2. Sample 250,000 values of each parameter $\{a, b, h, r, \gamma, u, v\}$ from the literature-based triangular distributions on Table 4.1, with the initial "SA init" values as the peak of each triangular distribution. No time-varying parameters T_i, k_i were selected, since by assumption the parameters are discrete functions of time. Triangular distributions were chosen as a best-guess approach that still allowed all possible values to occur.

3. For each subinterval, score each of the 250,000 parameter sets according to the error formula (Equation 4.1).

4. For each subinterval, collect the 100 best-performing parameter sets

4.3.1 China

The forest cover in China did not experience a pronounced transition between 1961 and 2010, because the rate of decline was never very steep. However, China did experience concurrent increases in forest and agricultural land, a phenomenon generally associated with forest transitions. This indicates dramatic increases in agricultural yields over this period, and substantial conversion of open land to other land covers; we expect v to be high in the latter half of this time series.

The results of the ensemble fitting approach confirm this suspicion. Estimates for the natural parameters are fairly consistent, as we had hoped, with minor exceptions for h and r. By contrast, there are large variations in the human parameters, including v in particular. Compared to other countries, the interquartile ranges (given by dotted lines) for a and r are quite wide, while those for u are quite narrow.

As the agricultural area expands, the estimated probability of long-term forest survival goes from unlikely to vanishingly remote. While the model suggested that reducing u was, by a small margin, the most effective choice to prevent forest collapse, in reality collapse appears to have been averted by only a slight decreases in u, and slight increases in γ and r. These were strong enough to offset the large increase in v.

Finally, the results of this discrete time parameter fitting are very different from those for the continuous time model. All the human parameter values are much higher in the discrete time model, and the large changes in the discrete time parameter values between [1976-1990] and [1986-2000] are barely reflected in the continuous model at all. Due to the smaller time intervals, the fits for the discrete time model are much more precise.

4.3.2 Costa Rica

Costa Rica had a very abrupt forest transition, which is a model of success in many areas of forest policy, including payment for ecosystem services [5]. As reported in Lambin and Meydfroidt, the forest cover data is of coarser quality, and has been generated by spline interpolation [10]. The model fits the data for Costa Rica less well than it did for China, since fits between 1970 and 1995 struggle to cope with the abruptness of the cusp in 1985.

This example is illustrative of the limitations of model retrodictions. Visually, it is clear that a forest transition occurs in 1985 (Figure 4.4). Even without seeing subsequent years of data, this discrete fitting approach would have shown a clear forest transition by 1990, as the forest cover outperforms the entire envelope of fitted model retrodictions. However, extrapolations do not show a decrease in collapse risk until 1995 (Figure 4.5),

when the forest transition has become clearly established. The model fits, and consequently the extrapolated steady states, are not as concave as the data, and only characterize a successful transition based on a more established trend.

Parameter estimates for Costa Rica are substantially more variable over time. The natural parameters are much less consistent, and the change in human parameters is more abrupt. There is a pronounced increase in estimates of r over time; this matches the onset of forest growth. Similarly, there are large decreases in b and u. Both γ and v have large spikes at the inflection point; γ regains its higher value, while v does not. The interquartile ranges are narrower for a and r than they are for China, while being quite large for v over most of the time series.

The initial decline is steep enough that all parameter estimates in the first several ensembles predict forest collapse; furthermore, none of the proposed interventions would be able to prevent this. Only in 1990 would any of these have an effect; u would be the strongest and γ the weakest. Five years later, parameters have already changed so substantially that all estimates predict stability.

Further illustrating the differences with the continuous model, the steady decline of u in this model fitting directly contradicts the continuous model fit of u increasing in the first decade and remaining high. However, one broad similarity can be found in the gradual increase in γ.

4.3.3 Vietnam

The forest transition in Vietnam was quite shallow, occurred late in the study period, and was unusually accompanied by an increase in agricultural land. Logically, this implies that open land must have been lost at a high rate to both forest and farmland.

Until about 1990, the parameter ensembles generated by the discrete time method remain static, and the forecast of collapse (which is already high, though easily prevented by reducing u) becomes gradually worse as forest cover continues to decrease. Following 1990, the agricultural abandonment rate γ declines sharply, while other parameters experience subtler changes: forest growth rate r increases, and forest conversion u, open land conversion v, and the natural disturbance b rate all decrease. Considering the net reduction in open land, it is surprising that v should decrease in this period; however, a net gain of farmland from open land is ensured by the large reduction in agricultural abandonment. The uncertainty on this agricultural abandonment rate is very high throughout.

The discrete time model is much better at describing the dynamics of land cover in

Vietnam than the continuous model, since the continuous model did not fit to the post-1990 forest transition.

4.3.4 Model robustness

To ensure that the conclusions of the previous sections were broadly valid, we tested the model under alternate conditions. First, we considered the model performance in a prediction task, rather than retrodiction. We fit the discrete-time model over 10-year windows (instead of 15) and plot the extrapolations over another 10 year period (Figures A.14-A.19). The estimated parameter values match very closely, but some of the same issues are apparent: in particular, calibration based on past data means that predictions do not accurately forecast increases in forest cover soon after the transition. In addition, we consider the impact of 25% and 75% changes in parameter values, and confirm that reducing the forest conversion rate u remains the best choice to decrease the risk of forest collapse.

4.4 Discussion

The results of both the continuous and discrete-time models show that reducing the forest conversion rate u is always a good candidate for averting collapse. It may be insufficient in many situations, but by comparison the relative effectiveness of increasing farmland abandonment or decreasing open land conversion are quite variable. This appears to contradict the findings of Chapter 3 that found greatest sensitivity to the agricultural abandonment rate γ. However, upon closer inspection, the findings show that the **initial** agricultural abandonment rate γ_0 is extremely important, but near the point of crisis the forest conversion rate u is more important. This did not emerge from the analysis of time-varying parameters in Chapter 3, because the variation in initial parameters meant that the time of intensification was arbitrary with respect to the actual system trajectory. In the real-world data of this chapter, that was not the case.

The continuous time model shows that forest transitions can occur from parameter combinations beyond those that might be suggested by forest transition theory [3]. The pattern of farmers consolidating high-quality land would suggest a decrease in u and/or v (as farmers cultivate less new land, and land abandonment outpaces new cultivation) followed by a decrease in γ (as they consolidate existing land). However, in Costa Rica, the only country for which the fitted model demonstrated a forest transition, the agricultural

abandonment rate increased substantially but remained high, without any other parameters adjusting to compensate. It may be that the end of the data period is still a transient, and a better fit would conform to a more classical pattern – or it may not.

The ensemble-based discrete time approach tells a different story for Costa Rica, which aligns more closely with the classical theory. Forest conversion declines steadily, and after a brief but significant spike, which enables the forest transition to occur, farmland abandonment returns to a baseline level only slightly higher than the pre-transition level.

The discrete time ensemble approach provides several advantages due to working over smaller subintervals. Over each subinterval, it naturally provides a much closer fit to the data, ensuring that the results accurately represent crucial periods of a forest transition. It can also function predictively in a limited capacity, with the ensemble approach generating probabilistic forecasts of forest collapse or stability based on recent trends. These forecasts can be used for strategically choosing which parameters to target to have the greatest impact on collapse risk. However, it is worth noting that the lack of feedback mechanisms (e.g. predicting a priori when demand for farmland is saturating) prevents this from being as effective a prediction tool as more integrated models might provide [4].

The discrete time ensemble approach has several disadvantages, too. A major one is that the estimated natural parameters are highly variable over time, which is not only unrealistic based on the model premises, but conceals a number of degrees of freedom. Conceptually, this can be fixed quite simply by forcing natural parameters to remain constant, but finding the best-fitting values (over the sum of errors of all subintervals, each with optimized human parameters) would be quite computationally intensive.

One novel feature of the ensemble approach to parameter fitting is that it introduces a meaningful measure of the value of information. If the value of one parameter is specified (say there is complete economic data on farmland abandonment that allows us to fix γ), then by inputting that value we can quantify the reduction in the variation of each other parameter.

Fitting our model to data using both the continuous-time simulated annealing approach and the discrete-time ensemble approach has provided some more insight into the functionality of this model (in that non-classical transitions are possible, and the timing of parameter changes need not coincide with the timing of regime changes), and provided situational awareness into the circumstances of forest transitions in China, Costa Rica, and Vietnam. As Vespignani argues for epidemic modelling, models provide not only forecasting, but situational awareness, intervention planning and projections, and the identification of factors that fundamentally alter the landscape [50]. Our previous bifurcation analysis and simulation work enabled some identification of fundamental factors. However, only by

applying the model to real data is it meaningful to talk about situational awareness and projections.

The discrete-time ensemble approach was partially developed due to the recognized lack of any other methods available to anticipate critical transitions. Its performance on this task is decidedly short-term, but can provide a meaningful risk assessment using the probability derived from an ensemble. The predicted collapses never arose, despite the fact that in each country the forecast suggested collapse was almost certain for over a decade. This is because the forecast was only extrapolating that such a collapse would happen eventually, and with the biased sample of three successful forest transitions, the parameters changed before the forest irrevocably crossed the threshold to collapse.

(a)

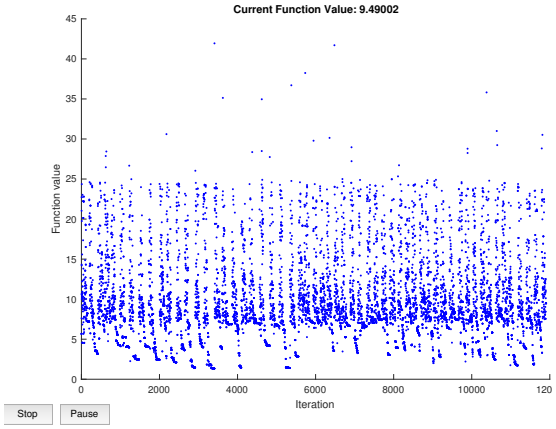

(b)

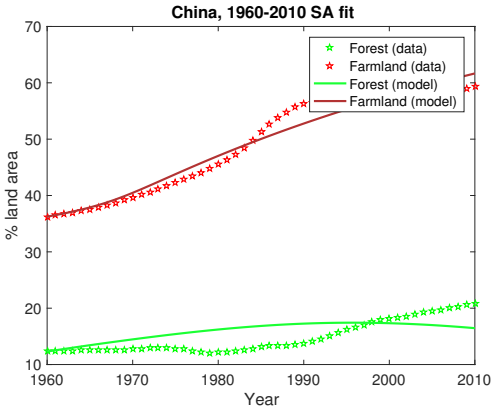

(c)

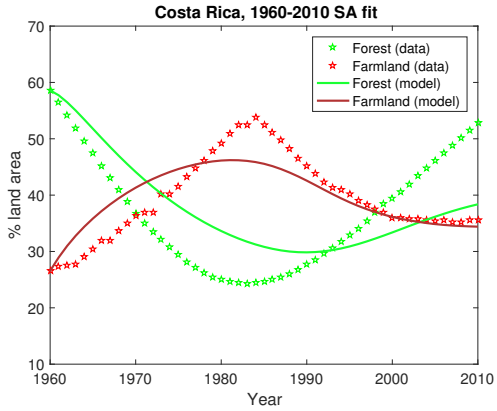

(d)

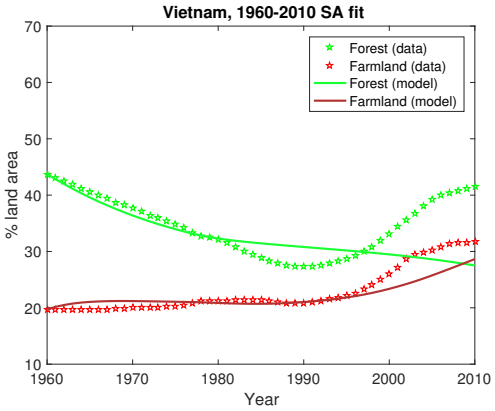

Figure 4.1: (a) Trace of simulated annealing algorithm for China. (b)-(d) Data and fitted continuous time model for China, Costa Rica, and Vietnam, respectively. The model captures broad trends very well, though it performs less well at capturing sudden shifts, such as Costa Rica's sharp forest transition or Vietnam's reforestation at the end of the data period.

Table 4.1: Parameter inputs and results for simulated annealing. "SA init", "SA min", and "SA max" define the inputs and bounds to the simulated annealing algorithm.

Term	Meaning	Units	SA init	SA min	SA max	China	Costa Rica	Vietnam
a	Low-density forest growth rate	% year^{-1}	1	0	10	6.85	6.66	3.64
b	Natural disturbance rate	% year^{-1}	2	0.5	26	2.10	1.57	8.64
h	Threshold for increased growth	%	15	10	50	25.82	19.20	10.22
p	Steepness of threshold (fixed)	–	3	3	3	3	3	3
r	High-density forest growth rate	% year^{-1}	40	2	50	23.45	39.49	14.52
T_γ	Time of change in γ	year	1980	1960	2010	1977.79	1988.96	1979.59
k_γ	Timescale of change in γ	years	5	1	10	7.75	3.89	9.85
γ_0	Initial agricultural abandonment rate	% year^{-1}	6	0.1	25	0.21	10.52	2.57
γ_1	Final agricultural abandonment rate	% year^{-1}	6	0.1	25	0.236	19.93	3.15
T_u	Time of change in u	year	1980	1960	2010	1962.01	1963.26	1961.09
k_u	Timescale of change in u	years	5	1	10	2.67	5.71	6.25
u_0	Initial forest conversion rate	% year^{-1}	4.5	0	25	0.446	4.58	0.459
u_1	Final forest conversion rate	% year^{-1}	1.8	0	25	1.23	8.88	0.409
T_v	Time of change in v	year	1980	1960	2010	1967.67	2007.80	1992.73
k_v	Timescale of change in v	years	5	1	10	2.23	1.62	2.14
v_0	Initial open land conversion rate	% year^{-1}	13	0	50	0.489	12.09	1.03
v_1	Final open land conversion rate	% year^{-1}	13	0	50	1.45	12.56	2.84

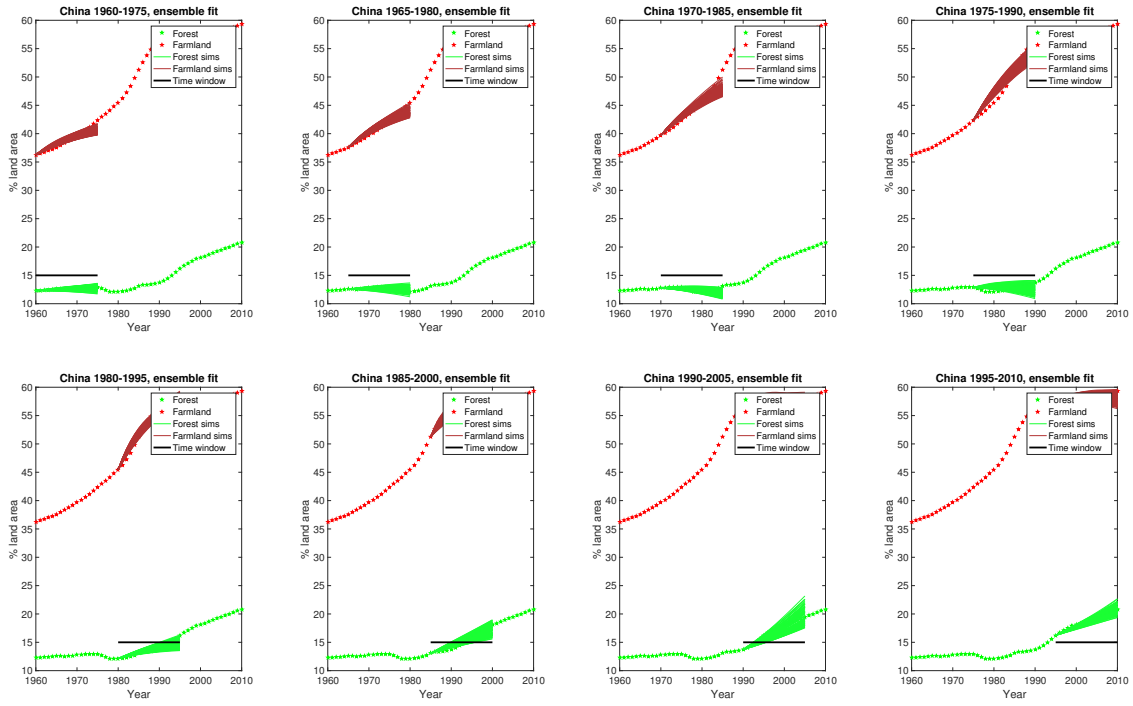

Figure 4.2: Fitted 15-year time windows for China. By updating parameter estimates every 5 years, these retrodictions match the data much more closely than in the continuous case. The same parameter estimates are also used to generate predictions of collapse risk (Figure 4.3). The period from 1980 to 1995 is particularly interesting, as forest begins to recover while agricultural land is still increasing, showing that these land uses are not always at odds.

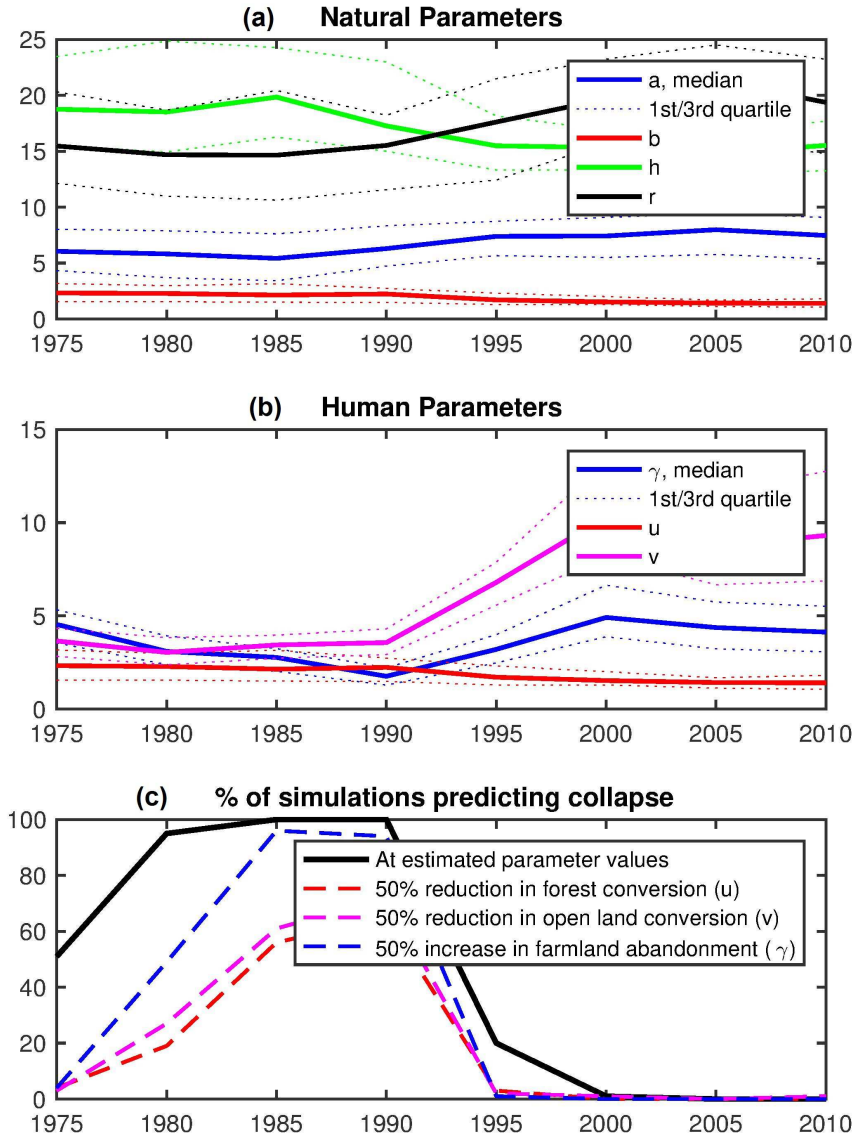

Figure 4.3: Fitted discrete-time parameter ensembles for China. Parameters were fitted over 15-year intervals; the axis indicates the final year of each interval (so "1975" covers 1961-1975). (a) Natural parameters. The fitted values remain relatively consistent, though wide interquartile ranges, particularly for h and r, indicate considerable uncertainty and/or a partially underdetermined model. (b) Human parameters. At the forest transition in 1990, open land conversion v increases substantially, but is mitigated by increased farmland abandonment and decreased forest conversion. (c) Extrapolations based on trends to date indicate that the risk of forest collapse virtually disappears between 1990 and 1995. Before collapse was averted, reducing u or v would have been most strategic.

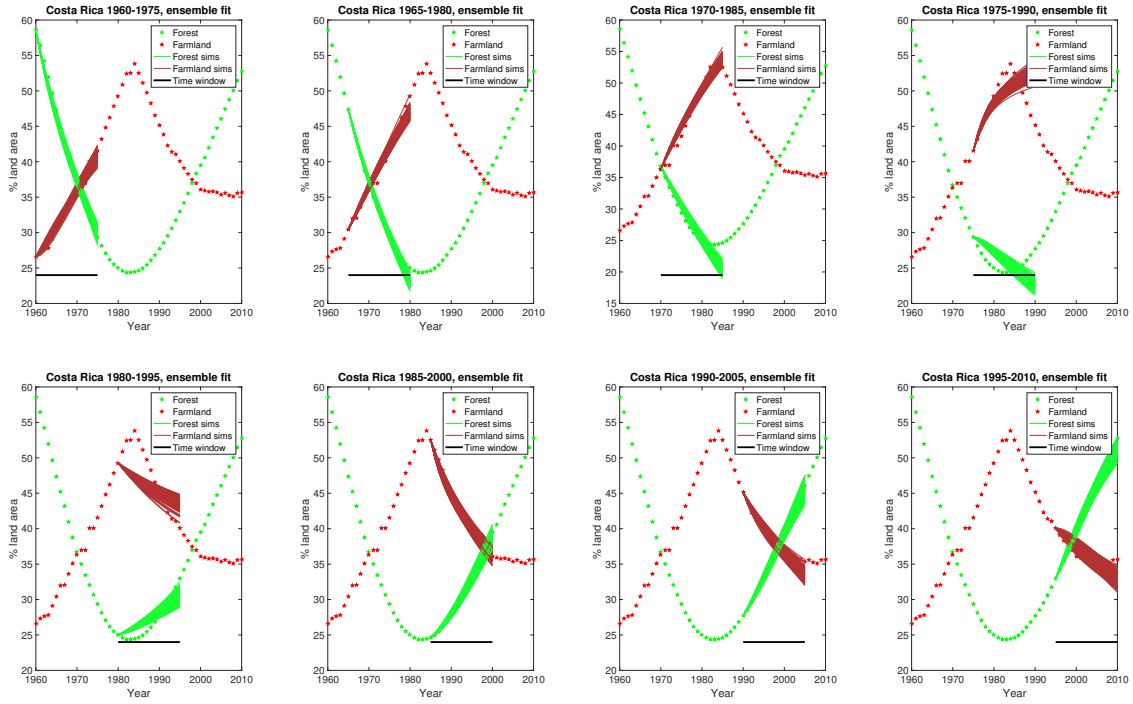

Figure 4.4: Fitted 15-year time windows for Costa Rica. These retrodictions fit the data for Costa Rica less well than they did for China, although this example is a more typical forest transition. Model fits covering the period between 1970 and 1995 show a discrepancy as improvements in forest cover occur faster than the model fitting window. The comparison of forest cover to model retrodictions allows us to identify a transition as early as 1985, 10 years before the extrapolated risk of collapse drops off (Figure 4.5); this difference occurs because it is only after 1995 that the transition is robust.

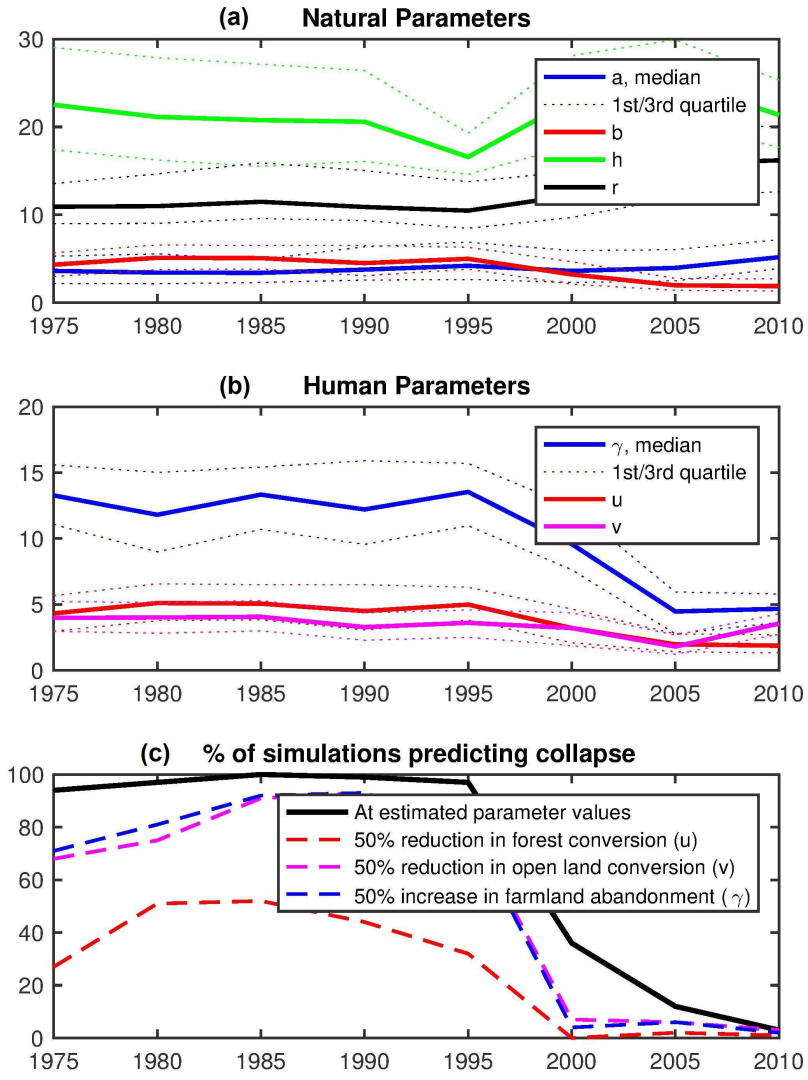

Figure 4.5: Fitted discrete-time parameter ensembles for Costa Rica. Parameters were fitted over 15-year intervals; the axis indicates the final year of each interval. (a) Natural parameters. The fitted values are much less consistent than they were for China. The best fitting threshold h declines as the forest cover declines; the estimated growth rate r increases as regrowth is observed. (b) Human parameters. Forest conversion u declines fairly steadily. Agricultural abandonment and to a lesser extent open land conversion have a large peak in the period [1975-1990], during the abrupt forest transition, followed by a return to their previous values. (c) Extrapolations based on trends to date provide little information in this case beyond an abrupt shift from certain collapse to certain forest persistence; this forest transition was very sudden.

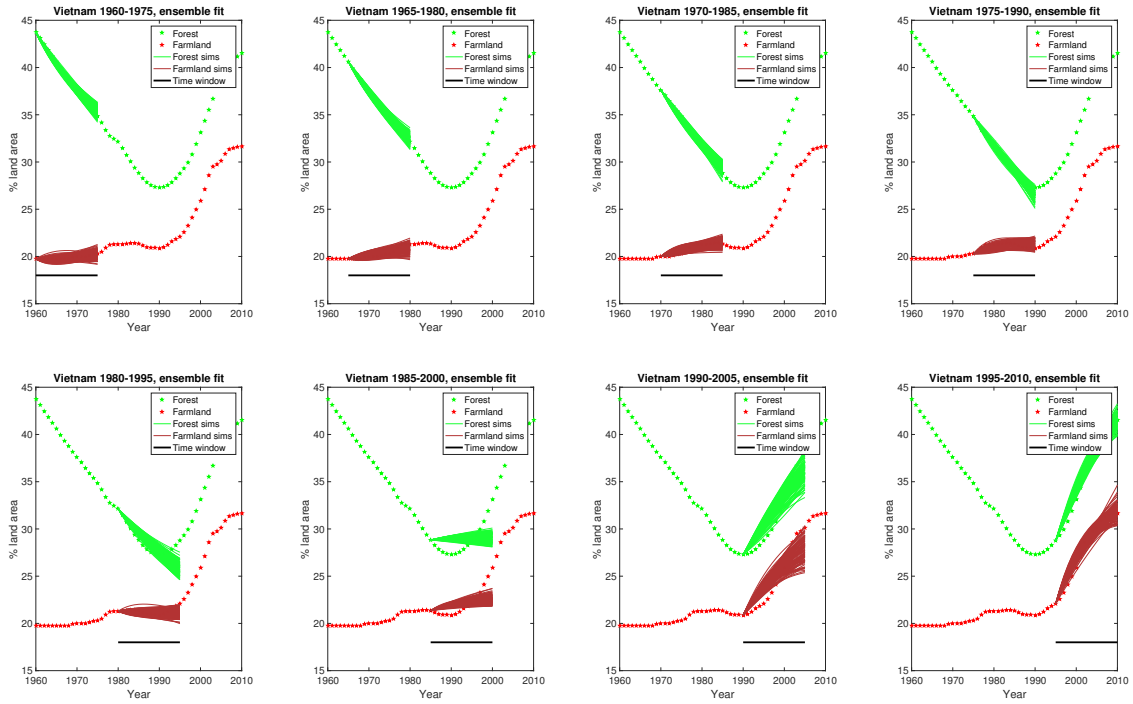

Figure 4.6: Fitted 15-year time windows for Vietnam. These retrodictions fit the data for Vietnam quite well, with the exception of the period 1985-2000. This discrepancy is due to the width of the fitting window. Unlike with Costa Rica, visual identification of forest transition timing (approximately 1995) matches the model's output (2000; Figure 4.7) reasonably closely. As with China, this shows an example of forest cover and agricultural land increasing simultaneously.

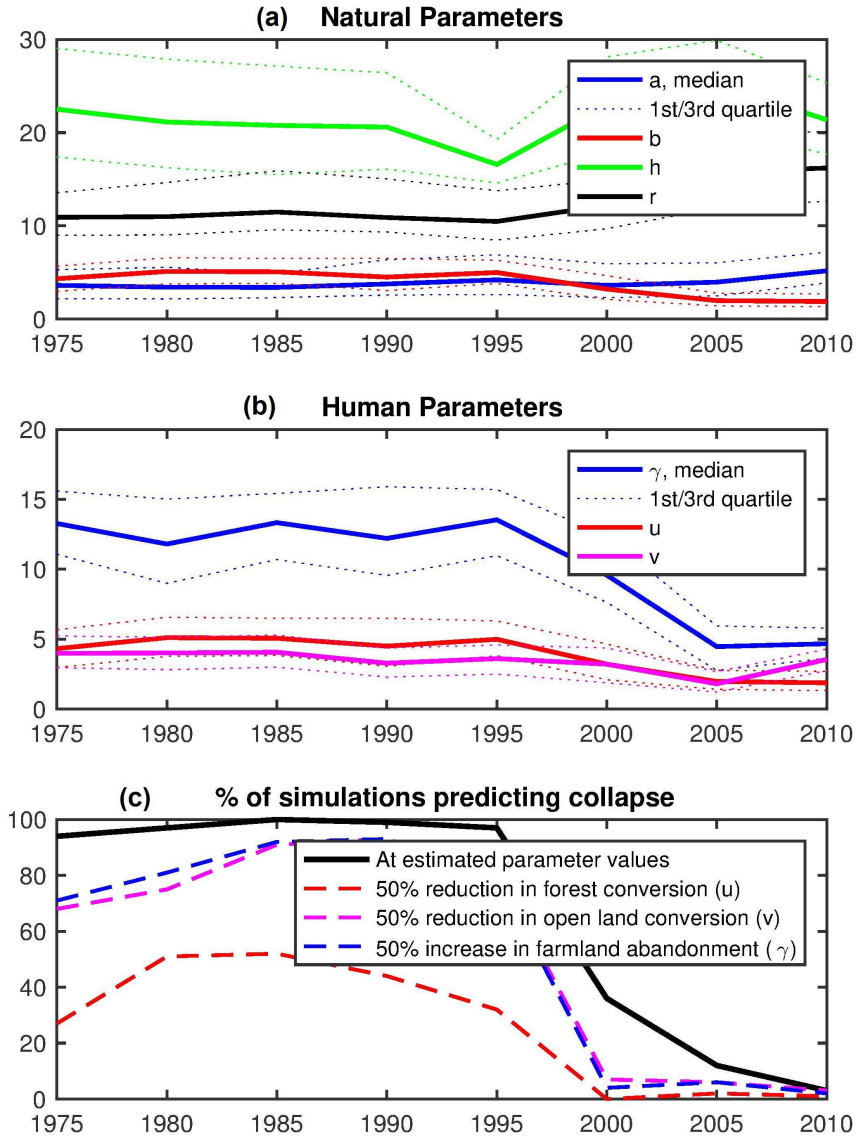

Figure 4.7: Fitted discrete-time parameter ensembles for Vietnam. Parameters were fitted over 15-year intervals; the axis indicates the final year of each interval. (a) Natural parameters. The fitted values are quite consistent over time, with the exception of a decline in b and a slight increase in r. The wide interquartile range reflects uncertainty. (b) Human parameters. Agricultural abandonment declines substantially, while the land conversion rates have a much smaller reduction; the net effect would be to destabilitze forest. (c) Contrary to the trends in estimated human parameters, extrapolations show that after 1995 the risk of forest collapse decreases significantly. Reducing u would have made a substantial impact on the risk of forest collapse right from 1975, unlike in the other countries.

Chapter 5

Summary and Discussion

5.1 Conclusions

We have developed a model that includes both ecological thresholds and forest transition dynamics, to synthesize the ideas of these often disparate research areas. Our general model can describe boreal or tropical forests, depending on parameter values, as found in previous literature. It includes explicit modeling of ecological thresholds and time-varying parameters, representing changing land use patterns as found in forest transition scenarios [35]. We have found that forest transitions may arise from patterns of parameter variation that are different from those predicted by theory; in particular, the agricultural abandonment rate may remain high rather than declining.

As expected [23], our analysis shows that pressures from agriculture may cause forests to collapse in a catastrophic shift [2], instead of merely declining as many forest transition models implicitly assume. For both tropical and boreal forests, we derive a critical forest cover level of around 20-25%. We have also shown that the risk of collapse is much more sensitive to agricultural parameters than to inherent forest parameters. The agricultural abandonment rate, in particular, has a strong, threshold-based effect: forest collapse almost never occurs if agricultural abandonment is greater than 10% annually. Sensitivity to forest conversion and open-land conversion is also high. In fact, in the real-world data sets we analyzed, decreasing the forest conversion rate would have been the most effective choice to minimize ecological damage and ensure earlier forest transitions.

The resilience metrics we used in Chapter 3 performed poorly, because at the outset of each simulation our system had no stable interior equilibrium. Therefore, methods based

on the characteristics (e.g. eigenvalues) of such an equilibrium were not applicable, and our analysis based on these metrics gave only limited post-hoc information. To predict potential collapses [24], we had to resolve this issue in a situation with unknown and time-varying parameters. We did by so by estimating ensembles of parameter sets over 15-year intervals and extrapolating the stable forest cover; this also allowed us to simulate interventions in various parameters.

From our analysis, we conclude that threshold-based models should be used much more often in the study of forest transitions. The possibility of forest (and other ecosystem) collapses should be a consideration in agricultural policies; it should be considered in addition to more linear measures such as remaining area or greenhouse gas emissions. One major consequence of this is that, even if a forest transition appears almost certain (due to projected agricultural intensification, planned replanting, or other factors), forest cover should not be permitted to decrease too far. In our model, this critical threshold would be 25%. As a more concrete example: if forest cover is currently 30%, and agricultural land cover is 60% but expected to decline to 45% within a few decades, then forest must still be protected, or ecological collapse may preclude a forest transition, even with favourable socio-economic conditions.

This is not to say that all models of the forest transition must necessarily incorporate ecological thresholds. Doing so would often add undesirable complexity, and would be plagued by technical difficulties, such as the difficulty accurately parameterizing the thresholds. However, researchers should be aware of the possibility of collapse, and consider it as a serious risk, particularly in the face of climate change. More broadly, stronger ties between forest transition research emphasizing socioeconomic factors and ecological research emphasizing nonlinear dynamics and critical transitions would be beneficial to both disciplines.

5.2 Limitations and directions for future work

The form of our model introduces numerous potential issues. In general, differential equation models of complicated systems sacrifice realism for interpretability [25]. For example, it is a strong assumption that forest growth occurs as an essentially mass-action process (i.e. with a rate given by the product of forest and open land). Land use change is an inherently spatial phenomenon; even if our non-spatial model can provide some insight, its results should be checked against agent-based or partial differential equation models.

Another limitation is that our model does not include any economic trade or socio-ecological feedback. The forest transition literature is largely concerned with economic

questions, such as trade balances of agricultural and forest products [5], which we did not include. Discussing trade between a number of countries or regions, each with their own potential forest transitions and ecological thresholds, would be an important extension of this work. Doing so could build a bridge from the local level on which ecological thresholds occur to the global level of feeding the world population and ensuring sufficient natural habitat [4]. Similarly, our model did not include feedback effects such as conservation-driven demand for forest; ecological dynamics are often coupled to social dynamics [29, 28]. In any case, future models should include socio-economic inputs to the land conversion rates.

Another major issue to be addressed is the issue of scale. In general, ecological feedbacks – particularly those severe enough to cause full ecosystem collapse – are best documented on small scales [2, 51]. Some tipping points in forest dynamics do occur on large scales [20], but in general these will not be the same national scales on which economic indicators and policy decisions occur. Even when large-scale thresholds in abundance data occur, such as tree cover densities in the entire boreal forest, the scale of any underlying feedback process is not clear [18]. Fundamentally, this thesis is based on investigating forest transitions under the hypothesis that ecological thresholds are present in the forest in question. They may not be: with Scotland's sub-5% forest cover for a period lasting a minimum of several decades [6], it is clear that there was no threshold to collapse. However, climate change may stress entire biomes, so new thresholds may emerge where there were none before [20, 23]. Models that include explicit moisture and/or temperature dependence [29, 23] are key tools in considering these questions. There are many difficulties in appropriately accounting for ecological thresholds, but it is important to keep them in mind when discussing the forest transition.

References

[1] Ontario Royal Commission. *Report of the Ontario Royal Commission on Forest Reservation and National Park*. Warwick and sons, March 1893.

[2] Marten Scheffer, Steve Carpenter, Jonathan A Foley, Carl Folke, and Brian Walker. Catastrophic shifts in ecosystems. *Nature*, 413(6856):591–596, 2001.

[3] Alexander S Mather and CL Needle. The forest transition: a theoretical basis. *Area*, 30(2):117–124, 1998.

[4] Chris Pagnutti, Chris T Bauch, and Madhur Anand. Outlook on a worldwide forest transition. *PloS one*, 8(10):e75890, 2013.

[5] Patrick Meyfroidt, Thomas K Rudel, and Eric F Lambin. Forest transitions, trade, and the global displacement of land use. *Proceedings of the National Academy of Sciences*, 107(49):20917–20922, 2010.

[6] AS Mather. Forest transition theory and the reforesting of scotland. *The Scottish Geographical Magazine*, 120(1-2):83–98, 2004.

[7] Christin Loran, Christian Ginzler, and Matthias Bürgi. Evaluating forest transition based on a multi-scale approach: forest area dynamics in switzerland 1850–2000. *Regional Environmental Change*, 16(6):1807–1818, 2016.

[8] Julien Wolfersberger, Philippe Delacote, and Serge Garcia. An empirical analysis of forest transition and land-use change in developing countries. *Ecological Economics*, 119:241–251, 2015.

[9] Ruth S DeFries, Thomas Rudel, Maria Uriarte, and Matthew Hansen. Deforestation driven by urban population growth and agricultural trade in the twenty-first century. *Nature Geoscience*, 3(3):178–181, 2010.

[10] Eric F Lambin and Patrick Meyfroidt. Global land use change, economic globalization, and the looming land scarcity. *Proceedings of the National Academy of Sciences*, 108(9):3465–3472, 2011.

[11] Patrick Meyfroidt and Eric F Lambin. Global forest transition: prospects for an end to deforestation. *Annual review of environment and resources*, 36, 2011.

[12] Edward B Barbier and Anteneh Tesfaw. Explaining forest transitions: The role of governance. *Ecological Economics*, 119:252–261, 2015.

[13] Akiko Satake and Thomas K Rudel. Modeling the forest transition: forest scarcity and ecosystem service hypotheses. *Ecological Applications*, 17(7):2024–2036, 2007.

[14] Max Rietkerk, Victor Brovkin, Peter M van Bodegom, Martin Claussen, Stefan C Dekker, Henk A Dijkstra, Sergey V Goryachkin, Pavel Kabat, Egbert H van Nes, Anje-Margriet Neutel, et al. Local ecosystem feedbacks and critical transitions in the climate. *Ecological Complexity*, 8(3):223–228, 2011.

[15] Anthony J Mills, Kevin H Rogers, Marc Stalmans, and Ed TF Witkowski. A framework for exploring the determinants of savanna and grassland distribution. *AIBS Bulletin*, 56(7):579–589, 2006.

[16] Carlo De Michele and Francesco Accatino. Tree cover bimodality in savannas and forests emerging from the switching between two fire dynamics. *PloS one*, 9(3):e91195, 2014.

[17] E Schertzer, AC Staver, and SA Levin. Implications of the spatial dynamics of fire spread for the bistability of savanna and forest. *Journal of mathematical biology*, 70(1-2):329–341, 2015.

[18] Marten Scheffer, Marina Hirota, Milena Holmgren, Egbert H Van Nes, and F Stuart Chapin. Thresholds for boreal biome transitions. *Proceedings of the National Academy of Sciences*, 109(52):21384–21389, 2012.

[19] JP Jasinski and Serge Payette. The creation of alternative stable states in the southern boreal forest, quebec, canada. *Ecological Monographs*, 75(4):561–583, 2005.

[20] Christopher PO Reyer, Niels Brouwers, Anja Rammig, Barry W Brook, Jackie Epila, Robert F Grant, Milena Holmgren, Fanny Langerwisch, Sebastian Leuzinger, Wolfgang Lucht, et al. Forest resilience and tipping points at different spatio-temporal scales: approaches and challenges. *Journal of Ecology*, 103(1):5–15, 2015.

[21] Marina Hirota, Milena Holmgren, Egbert H Van Nes, and Marten Scheffer. Global resilience of tropical forest and savanna to critical transitions. *Science*, 334(6053):232–235, 2011.

[22] Egbert H Nes, Marina Hirota, Milena Holmgren, and Marten Scheffer. Tipping points in tropical tree cover: linking theory to data. *Global change biology*, 20(3):1016–1021, 2014.

[23] Arie Staal, Stefan C Dekker, Marina Hirota, and Egbert H van Nes. Synergistic effects of drought and deforestation on the resilience of the south-eastern amazon rainforest. *Ecological Complexity*, 22:65–75, 2015.

[24] Marten Scheffer, Jordi Bascompte, William A Brock, Victor Brovkin, Stephen R Carpenter, Vasilis Dakos, Hermann Held, Egbert H Van Nes, Max Rietkerk, and George Sugihara. Early-warning signals for critical transitions. *Nature*, 461(7260):53–59, 2009.

[25] Leah Edelstein-Keshet. *Mathematical models in biology*. SIAM, 2005.

[26] Yuri A Kuznetsov. *Elements of applied bifurcation theory*, volume 112. Springer Science & Business Media, 2013.

[27] Matthew C Hansen, Peter V Potapov, Rebecca Moore, Matt Hancher, SA Turubanova, Alexandra Tyukavina, David Thau, SV Stehman, SJ Goetz, TR Loveland, et al. High-resolution global maps of 21st-century forest cover change. *science*, 342(6160):850–853, 2013.

[28] Clinton Innes, Madhur Anand, and Chris T Bauch. The impact of human-environment interactions on the stability of forest-grassland mosaic ecosystems. *Scientific reports*, 3, 2013.

[29] Kirsten A. Henderson. *Alternative stable states and human-environment interactions in forest mosaics and ecotones*. PhD thesis, University of Guelph, 2016.

[30] Joana Figueiredo and Henrique M Pereira. Regime shifts in a socio-ecological model of farmland abandonment. *Landscape ecology*, 26(5):737–749, 2011.

[31] Paul E Waggoner and Jesse H Ausubel. How much will feeding more and wealthier people encroach on forests? *Population and Development Review*, 27(2):239–257, 2001.

[32] Acevedo W. Auch R.F. Sohl T.L. Drummond M.A. Sleeter B.M. Sorenson D.G. Kambly S. Wilson T.S. Taylor J.L. Sayler K.L. Stier M.P. Barnes C.A. Methven S.C. Loveland T.R. Headley R. Soulard, C.E. and M.S. Brooks. *Land cover trends dataset, 1973-2000*. U.S. Geological Survey Data Series, 2014.

[33] Jefferson Fox, Dao Minh Truong, A Terry Rambo, Nghiem Phuong Tuyen, Le Trong Cuc, and Stephen Leisz. Shifting cultivation: a new old paradigm for managing tropical forests. *BioScience*, 50(6):521–528, 2000.

[34] Glen W Armstrong. A stochastic characterisation of the natural disturbance regime of the boreal mixedwood forest with implications for sustainable forest management. *Canadian Journal of Forest Research*, 29(4):424–433, 1999.

[35] Alexander S Mather. The forest transition. *Area*, pages 367–379, 1992.

[36] Jonathan A Foley, Navin Ramankutty, Kate A Brauman, Emily S Cassidy, James S Gerber, Matt Johnston, Nathaniel D Mueller, Christine O'Connell, Deepak K Ray, Paul C West, et al. Solutions for a cultivated planet. *Nature*, 478(7369):337–342, 2011.

[37] Alexander V Prishchepov, Daniel Müller, Maxim Dubinin, Matthias Baumann, and Volker C Radeloff. Determinants of agricultural land abandonment in post-soviet european russia. *Land use policy*, 30(1):873–884, 2013.

[38] Peter Potapov, Matthew C Hansen, Stephen V Stehman, Thomas R Loveland, and Kyle Pittman. Combining modis and landsat imagery to estimate and map boreal forest cover loss. *Remote Sensing of Environment*, 112(9):3708–3719, 2008.

[39] Sean M McMahon, Geoffrey G Parker, and Dawn R Miller. Evidence for a recent increase in forest growth. *Proceedings of the National Academy of Sciences*, 107(8):3611–3615, 2010.

[40] L. D'Orangeville, L. Duchesne, D. Houle, D. Kneeshaw, B. Côté, and N. Pederson. Northeastern north america as a potential refugium for boreal forests in a warming climate. *Science*, 352(6292):1452–1455, 2016.

[41] Richard Fuchs, Martin Herold, Peter H Verburg, Jan GPW Clevers, and Jonas Eberle. Gross changes in reconstructions of historic land cover/use for europe between 1900 and 2010. *Global change biology*, 21(1):299–313, 2015.

[42] Fernando DB Espírito-Santo, Manuel Gloor, Michael Keller, Yadvinder Malhi, Sassan Saatchi, Bruce Nelson, Raimundo C Oliveira Junior, Cleuton Pereira, Jon Lloyd, Steve Frolking, et al. Size and frequency of natural forest disturbances and the amazon forest carbon balance. *Nature communications*, 5, 2014.

[43] Natural Resources Canada. Sustainable forest management in canada.

[44] Alan Hastings. Transients: the key to long-term ecological understanding? *Trends in Ecology & Evolution*, 19(1):39–45, 2004.

[45] Environment Canada. *How Much Habitat is Enough?* Environment Canada, 3rd edition, 2013.

[46] Chris T Bauch, Ram Sigdel, Joe Pharaon, and Madhur Anand. Early warning signals of regime shifts in coupled human–environment systems. *Proceedings of the National Academy of Sciences*, page 201604978, 2016.

[47] Brian Walker, Crawford S Holling, Stephen Carpenter, and Ann Kinzig. Resilience, adaptability and transformability in social–ecological systems. *Ecology and society*, 9(2), 2004.

[48] Katharine N Suding, Katherine L Gross, and Gregory R Houseman. Alternative states and positive feedbacks in restoration ecology. *Trends in Ecology & Evolution*, 19(1):46–53, 2004.

[49] Food and Agriculture Organization of the United Nations. Faostat database, 2015.

[50] *Proceedings of the IV AMMCS International Conference (Waterloo, Canada, August 2017).*

[51] Santa Fe Institute Resiliance Alliance. Thresholds and alternate states in ecological and social-ecological systems.

Appendix A

Appendix

Code for all figures in this thesis is stored at this repository:

https://ln.sync.com/dl/223975570/be3famsy-5224977q-srtak6cu-nynx2n8z.

This includes a list of the scripts produce each of the figures in the thesis.

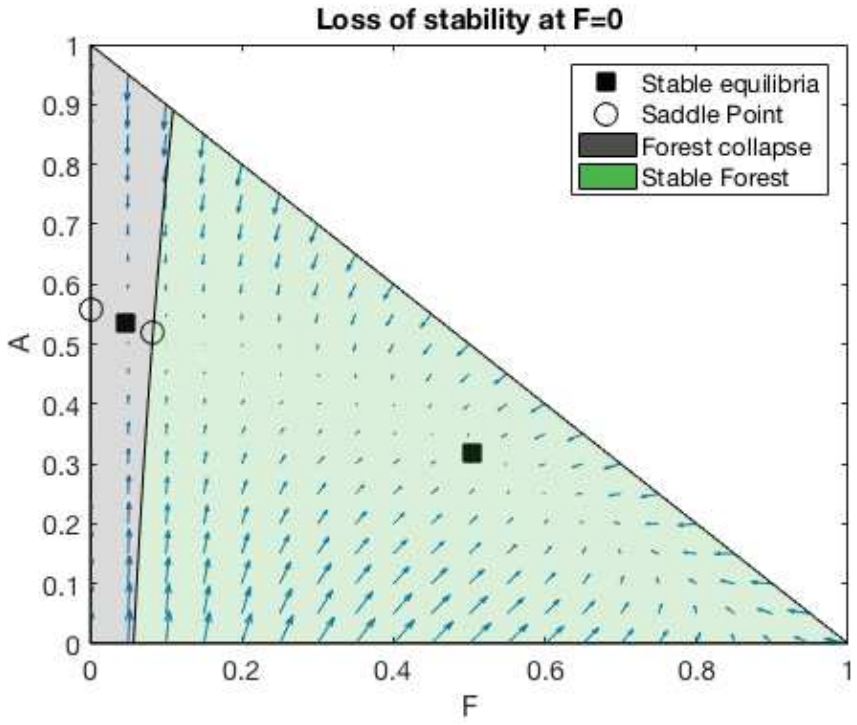

Figure A.1: Loss of stability at the $F = 0$ equilibrium. Instead, $F = 0$ is a saddle point, and there are two stable interior equilibria, corresponding to high and low forest cover. Parameters are $a = 3.74, b = 1.15, h = 20.68, p = 3, r = 11.91, \gamma = 9.76, u = 1.29, v = 4.96$.

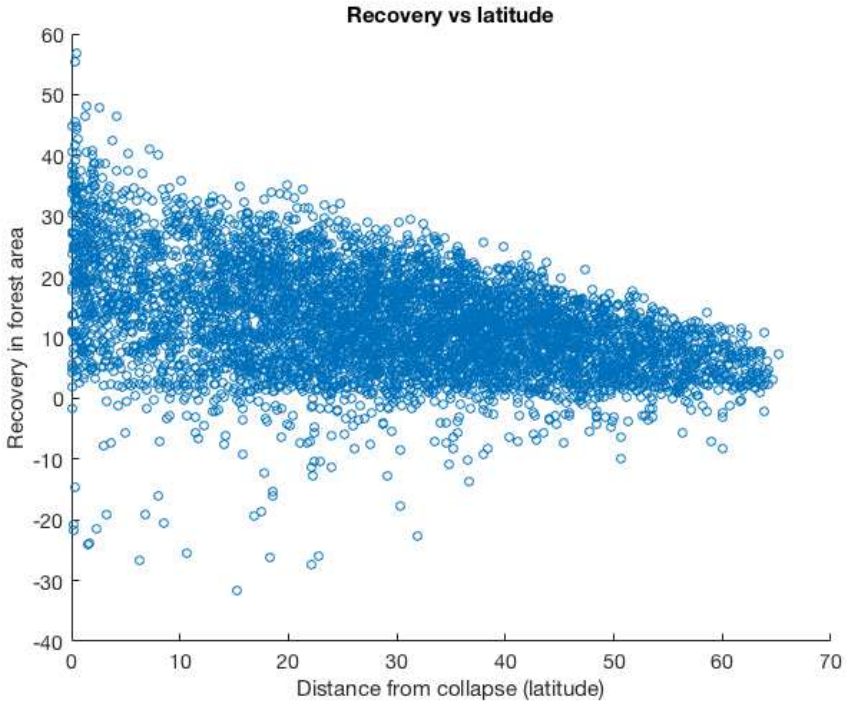

Figure A.2: Relationship between recovery (% forest cover regained) and latitude (minimum distance from collapse). Situations that never approach collapse cannot experience large recoveries, but otherwise there is no strong association.

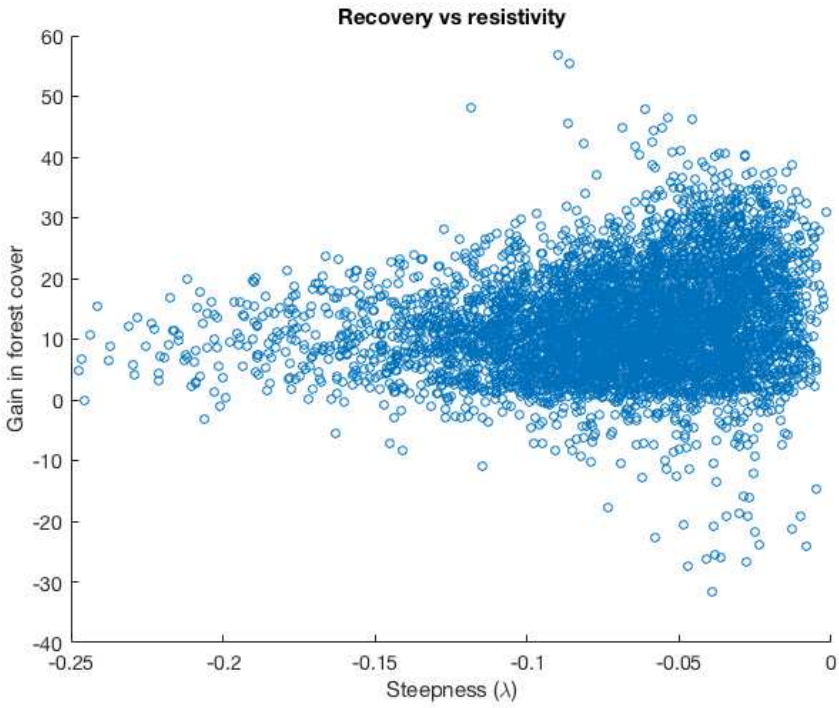

Figure A.3: Relationship between recovery (% forest cover regained) and resistance (λ, the dominant eigenvalue of the interior equilibrium). Strongly stable systems do not experience large recoveries, since they do not decline. For weakly stable systems, there is no strong association, and the extent of recovery is highly variable.

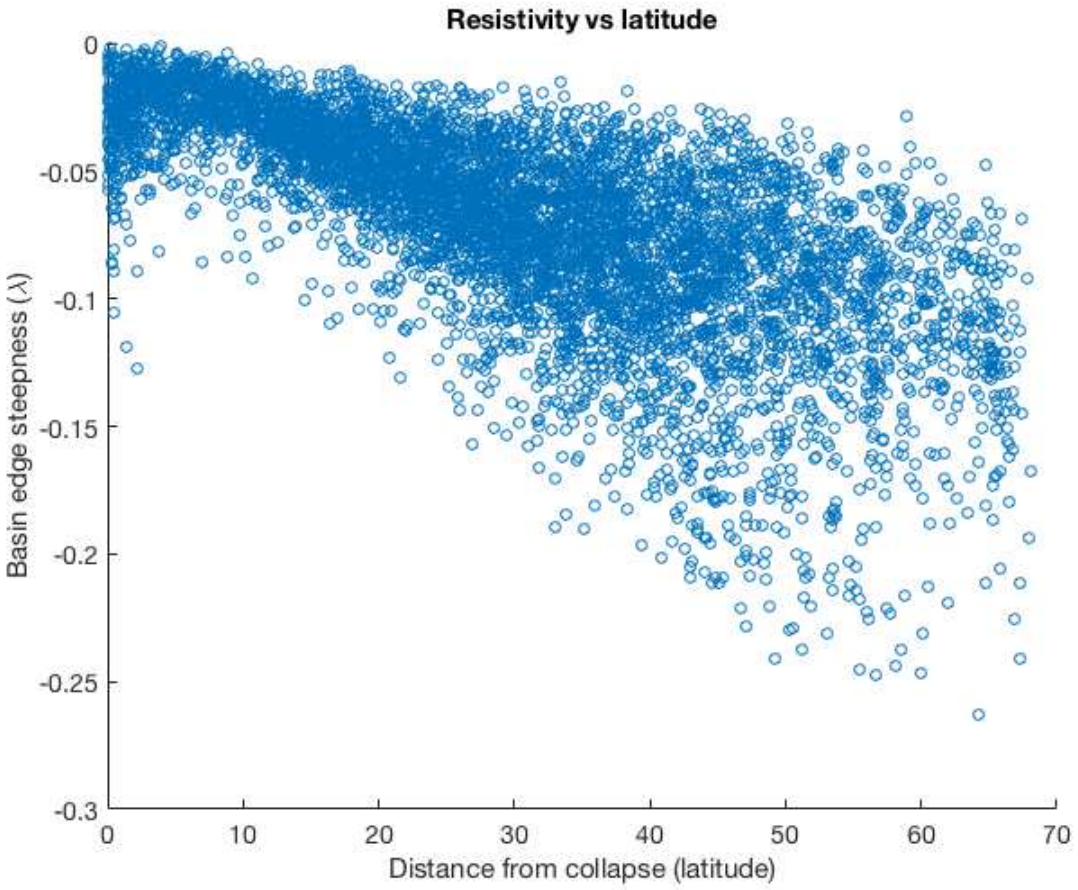

Figure A.4: Relationship between resistance (λ, the dominant eigenvalue of the interior equilibrium) and latitude (minimum distance from collapse). The correlation between these two resilience measures is stronger than it was between either of them and forest recovery. Broadly, simulations that were further from collapse were also more resistant to perturbations. One exception is in the upper left of this graph, with a a cluster of points that come very near to collapse yet are reasonably resistant to disturbances.

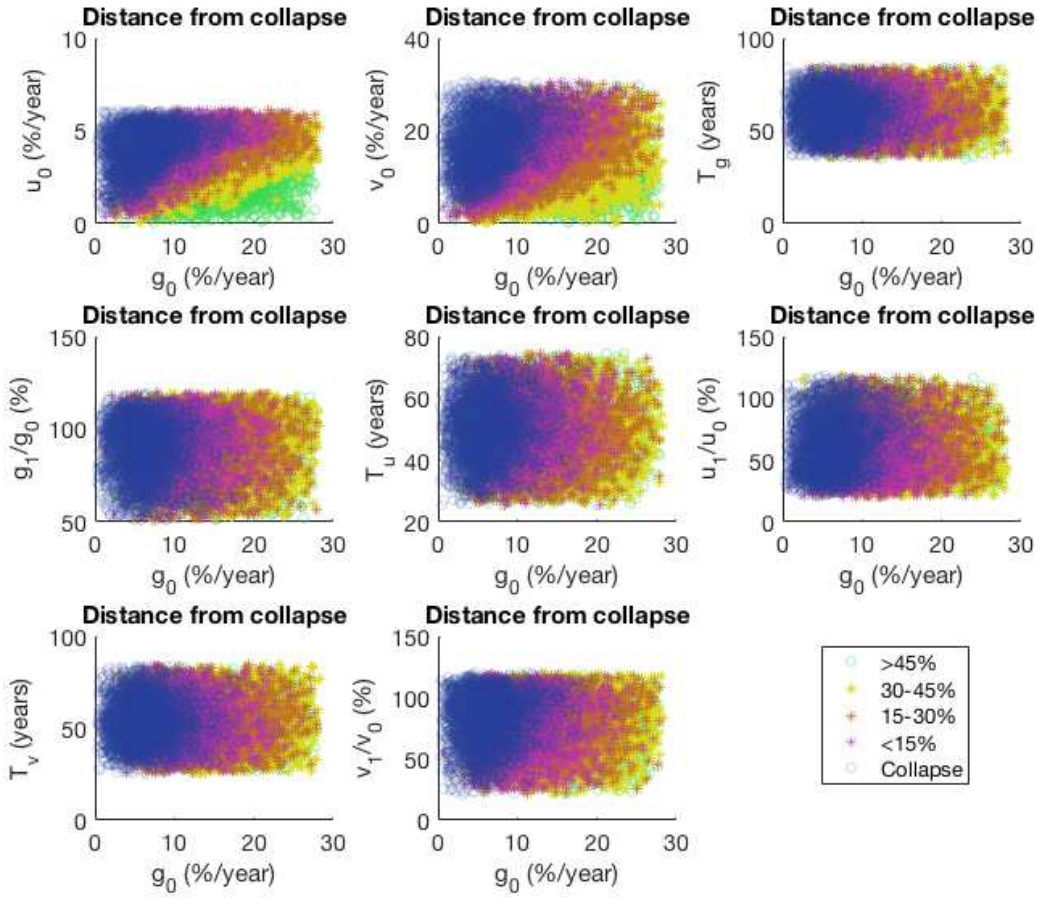

Figure A.5: Cross-effects of γ_0 and other parameters on distance from collapse. There are strong cross-effects with u_0 and v_0, but interactions with other parameters, including the time of intensification T_γ are much weaker.

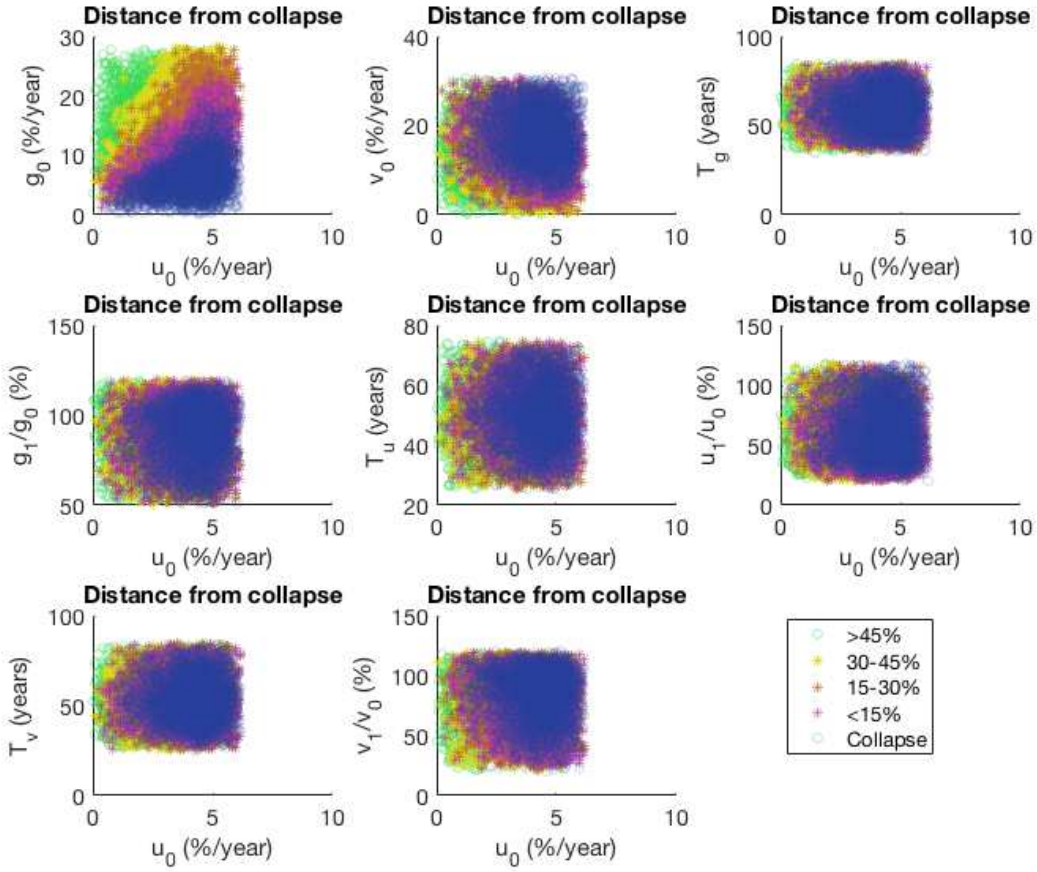

Figure A.6: Cross-effects of u_0 and other parameters on distance from collapse. There are strong cross-effects with γ_0 and v_0, but interactions with other parameters, including the time of intensification T_u, are much weaker.

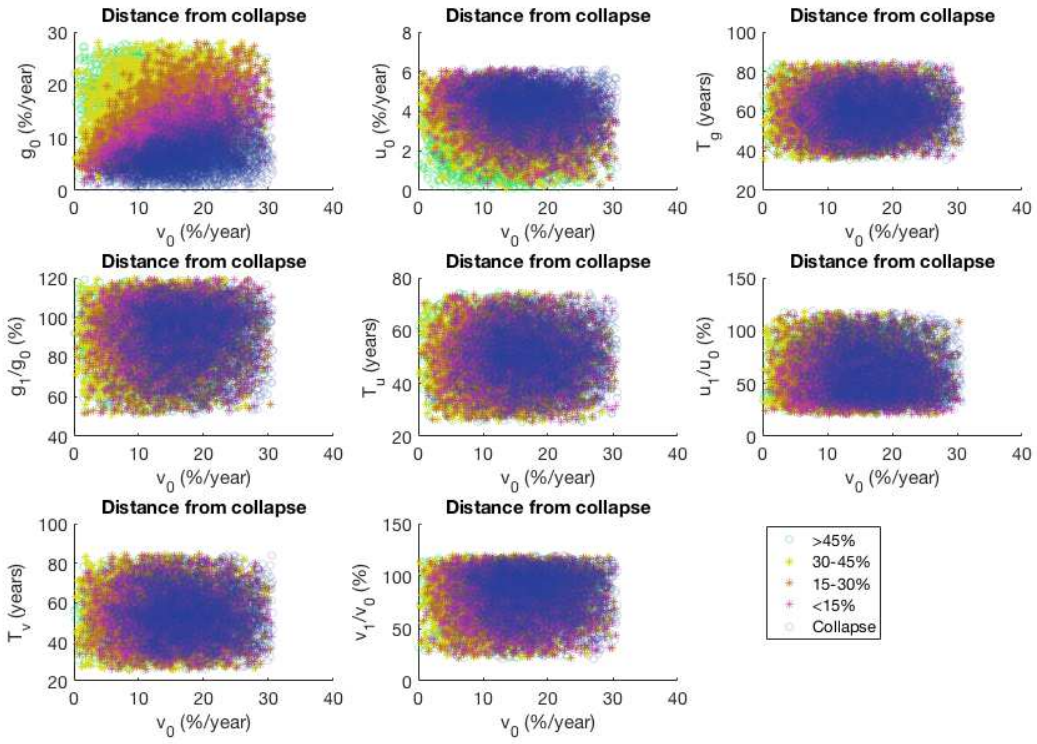

Figure A.7: Cross-effects of open land conversion rate v and other parameters on distance from collapse. There are strong interdependencies with the dominant parameters γ and u, and little interaction with other parameters, including T_v, the time of intensification of open land conversion.

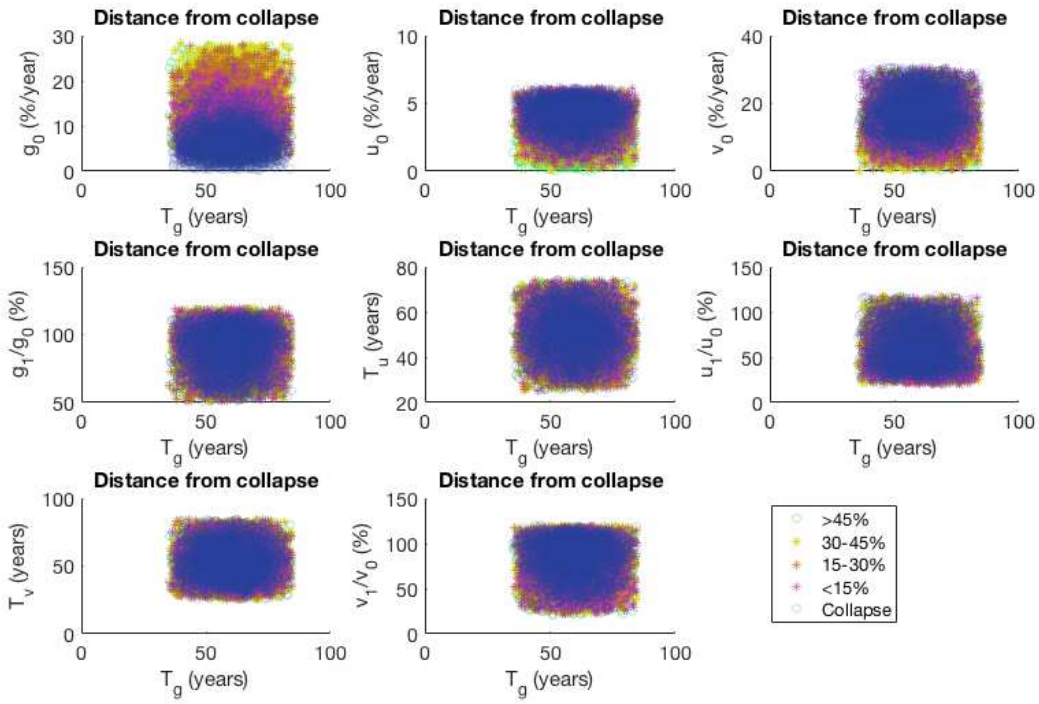

Figure A.8: Cross-effects of T_γ and other parameters on distance from collapse. The first-order effects of the dominant parameters γ_0, u_0, v_0 are visible, but T_γ does not display strong interactions with any parameters, including the magnitude of the shift in γ. This shows how weak the effect of land-use intensification is on resilience.

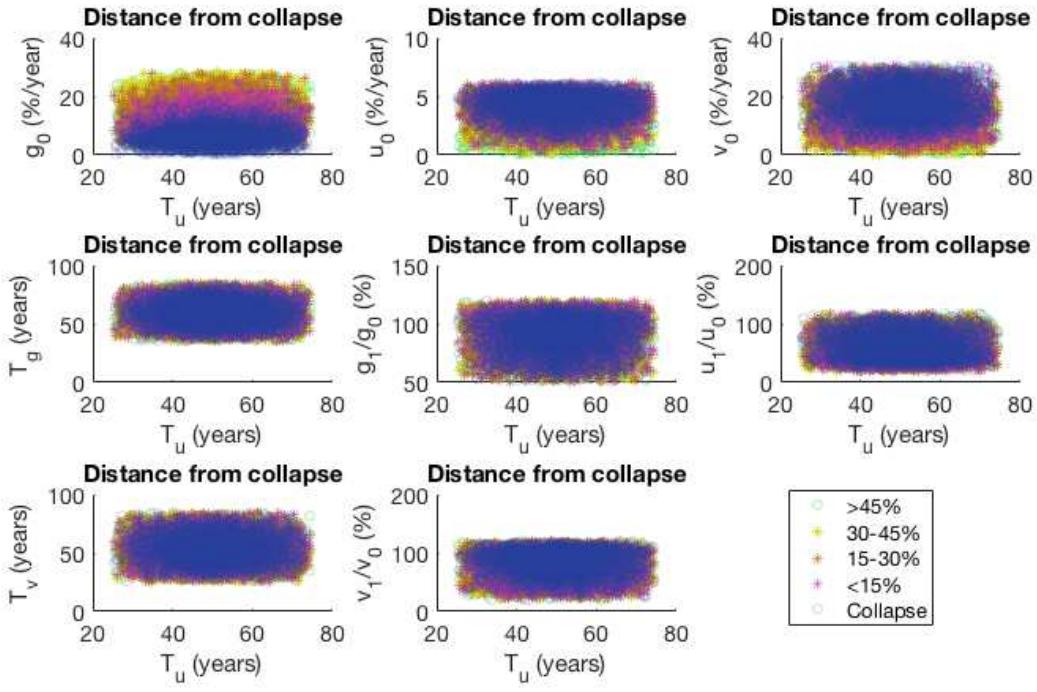

Figure A.9: Cross-effects of T_u and other parameters on distance from collapse. The first-order effects of the dominant parameters γ_0, u_0, v_0 are visible, but T_u does not display strong interactions with any parameters, including the magnitude of the shift in u. This shows how weak the effect of land-use intensification is on resilience.

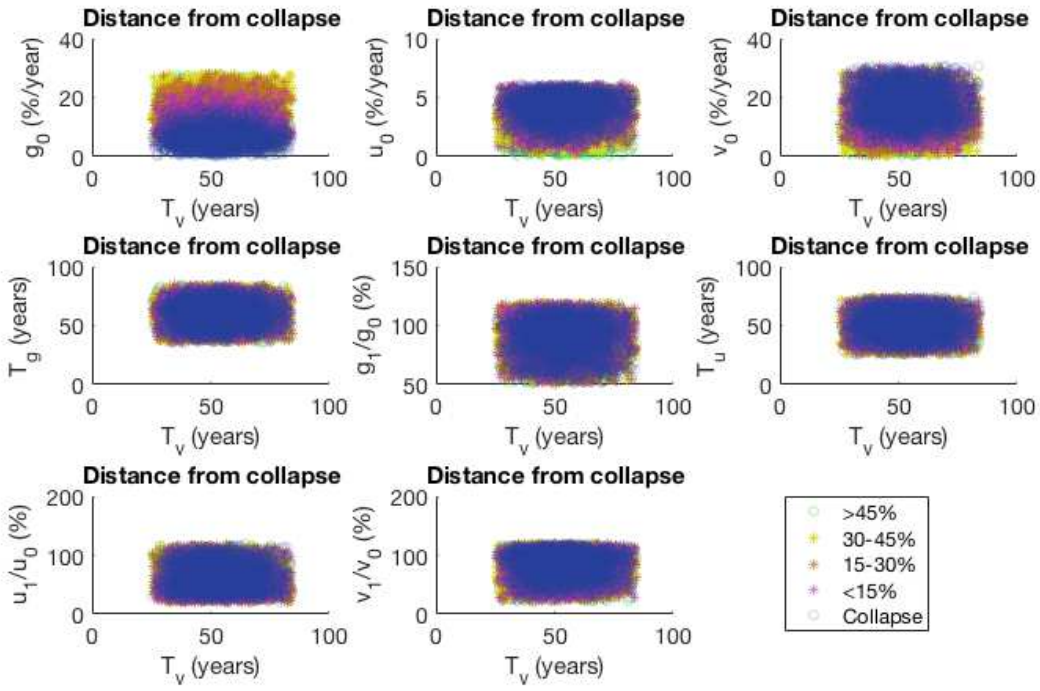

Figure A.10: Cross-effects of T_v and other parameters on distance from collapse. The first-order effects of the dominant parameters γ_0, u_0, v_0 are visible, but T_v does not display strong interactions with any parameters, including the magnitude of the shift in v. This shows how weak the effect of land-use intensification is on resilience.

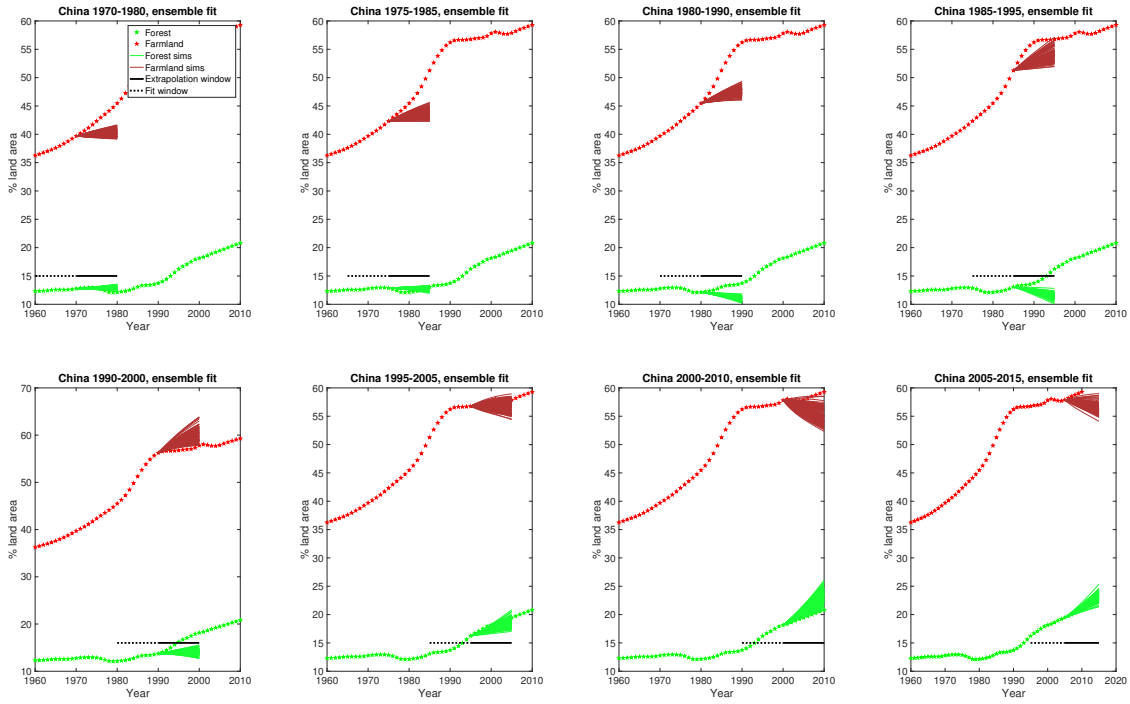

Figure A.11: 10 year prediction windows for China. We use the same discrete-time model as Figure 4.2 to make short-term forecasts, instead of simply retrodiction. Overall the ensembles perform well, but often underestimates agricultural land and does not predict the increase in forest cover after 1990.

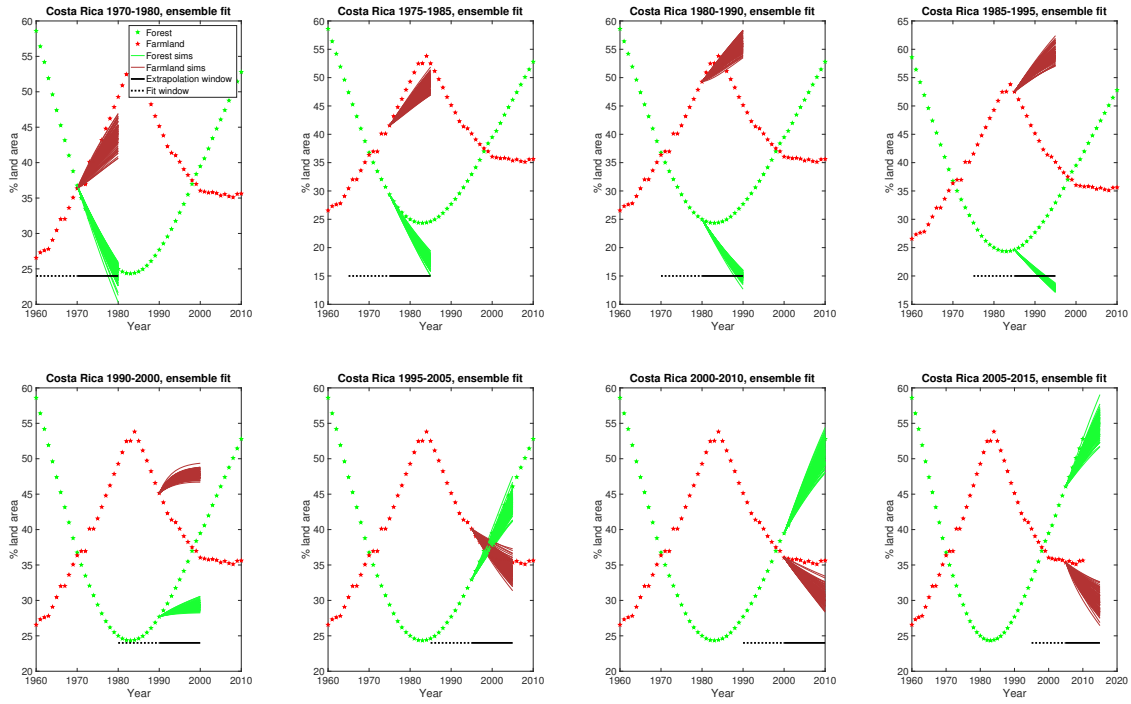

Figure A.12: 10 year prediction windows for Costa Rica. We use the same discrete-time model as Figure 4.2 to make short-term forecasts, instead of simply retrodiction. Due to the reliance on past data, forecasts show continued decline (or mediocre recovery) even when a robust recovery is under way.

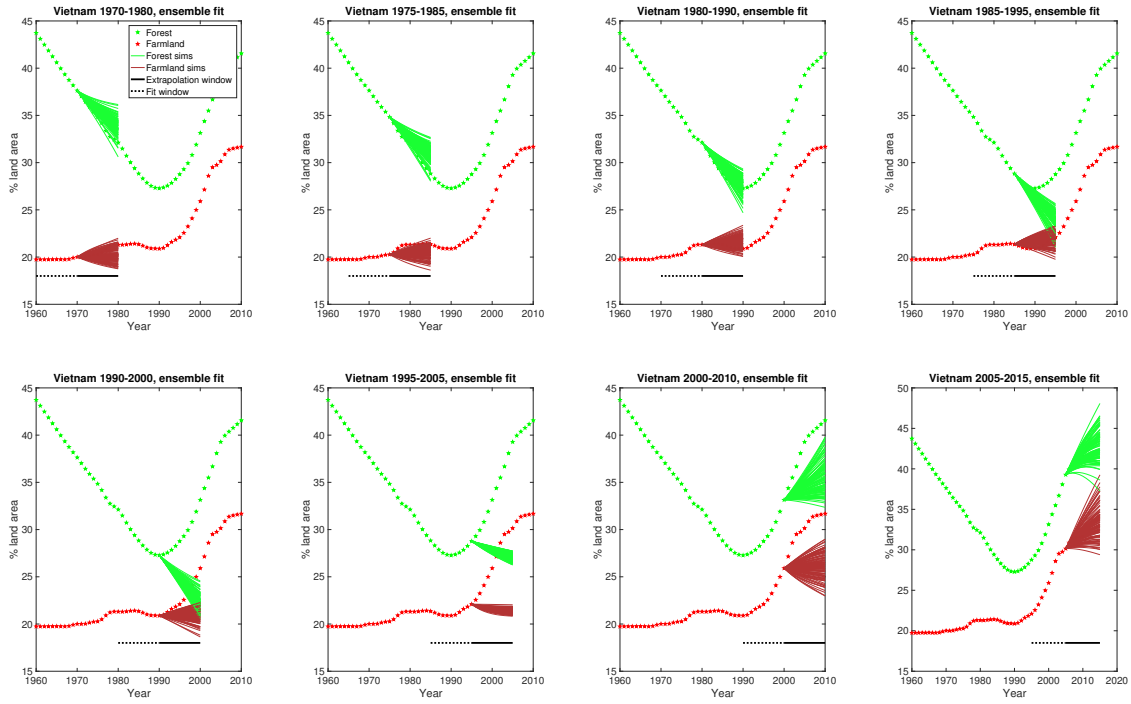

Figure A.13: 10 year prediction windows for Vietnam. We use the same discrete-time model as Figure 4.2 to make short-term forecasts, instead of simply retrodiction. Some of the same issues are present around the failure to predict recovery, but this example is particularly interesting for the considerable increase in uncertainty after 2005.

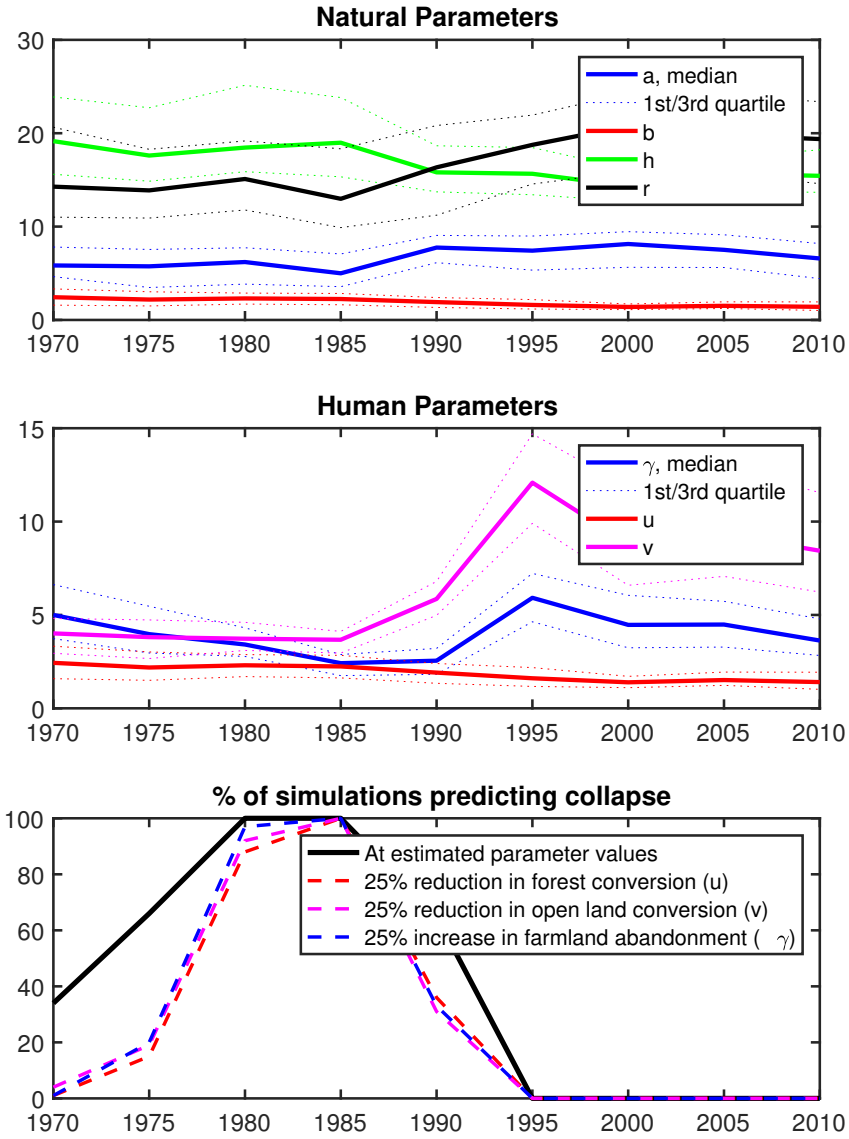

Figure A.14: Fitted discrete-time parameter ensembles for China with 25% reduction. The upper and middle panels reproduce the results of Figure 4.3, though fitted over 10 years instead of 15, confirming that the results are not sensitive to the fitting window. The bottom subpanel shows that for a 25% change in parameters, reducing u still produces the best results.

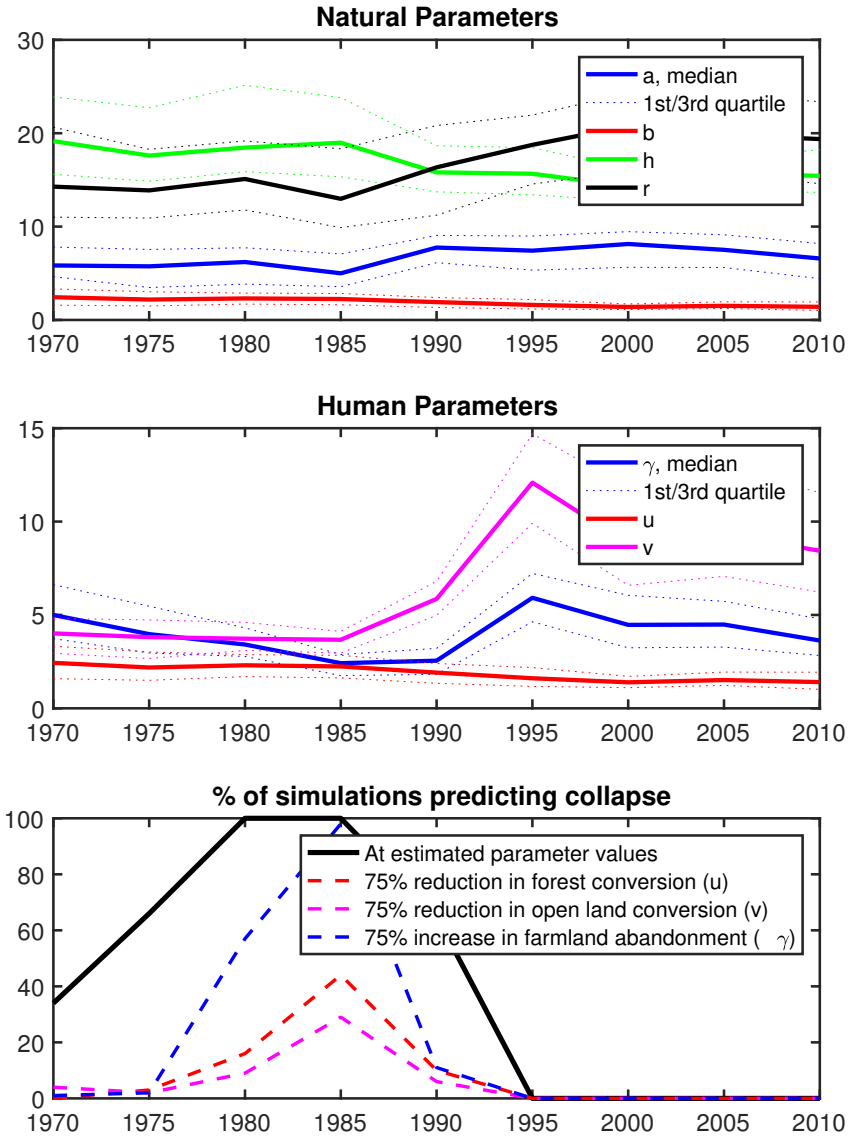

Figure A.15: Fitted discrete-time parameter ensembles for China with 75% reduction. The upper and middle panels reproduce the results of Figure 4.3, though fitted over 10 years instead of 15, confirming that the results are not sensitive to the fitting window. The bottom subpanel shows that for a 75% change in parameters, reducing u still produces the best results.

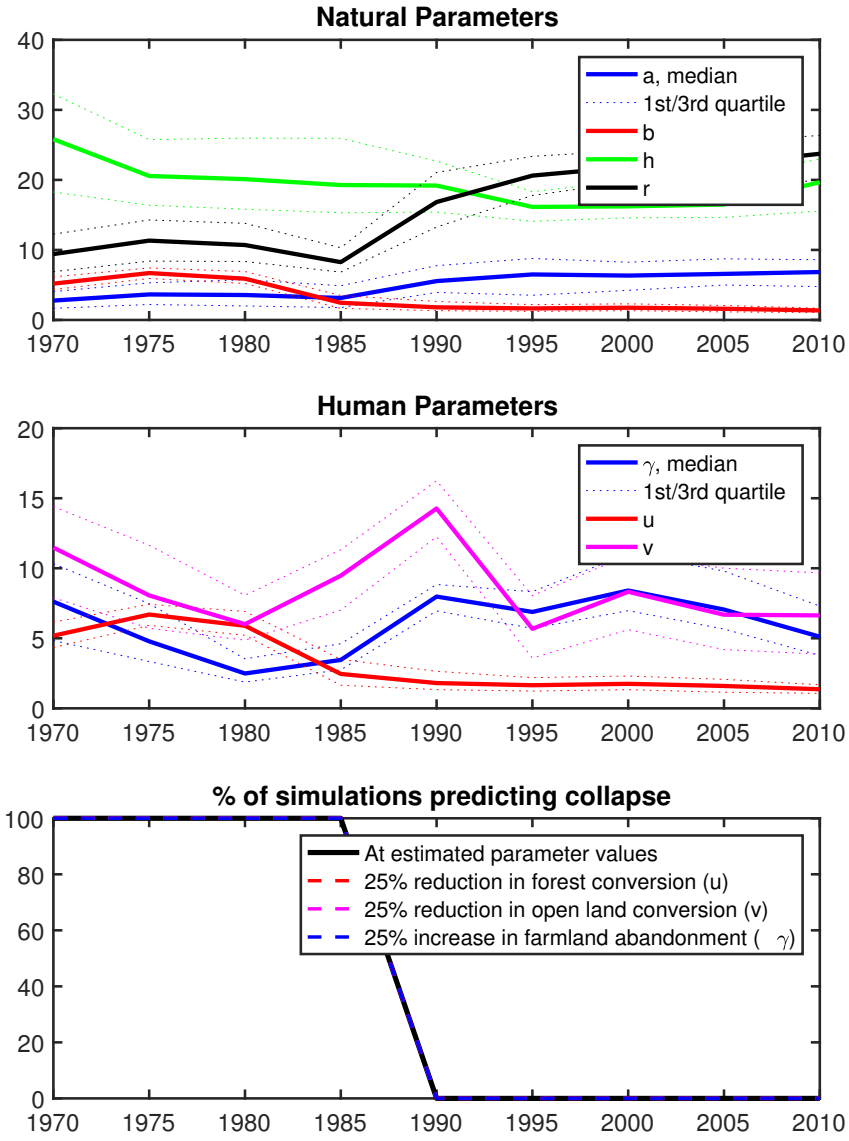

Figure A.16: Fitted discrete-time parameter ensembles for Costa Rica with 25% reduction. The upper and middle panels reproduce the results of Figure 4.5, though fitted over 10 years instead of 15, confirming that the results are not sensitive to the fitting window. The bottom subpanel shows that for a 25% change in parameters, no reduction in collapse risk can be achieved. There is as much reason to reduce u as to change any other parameter.

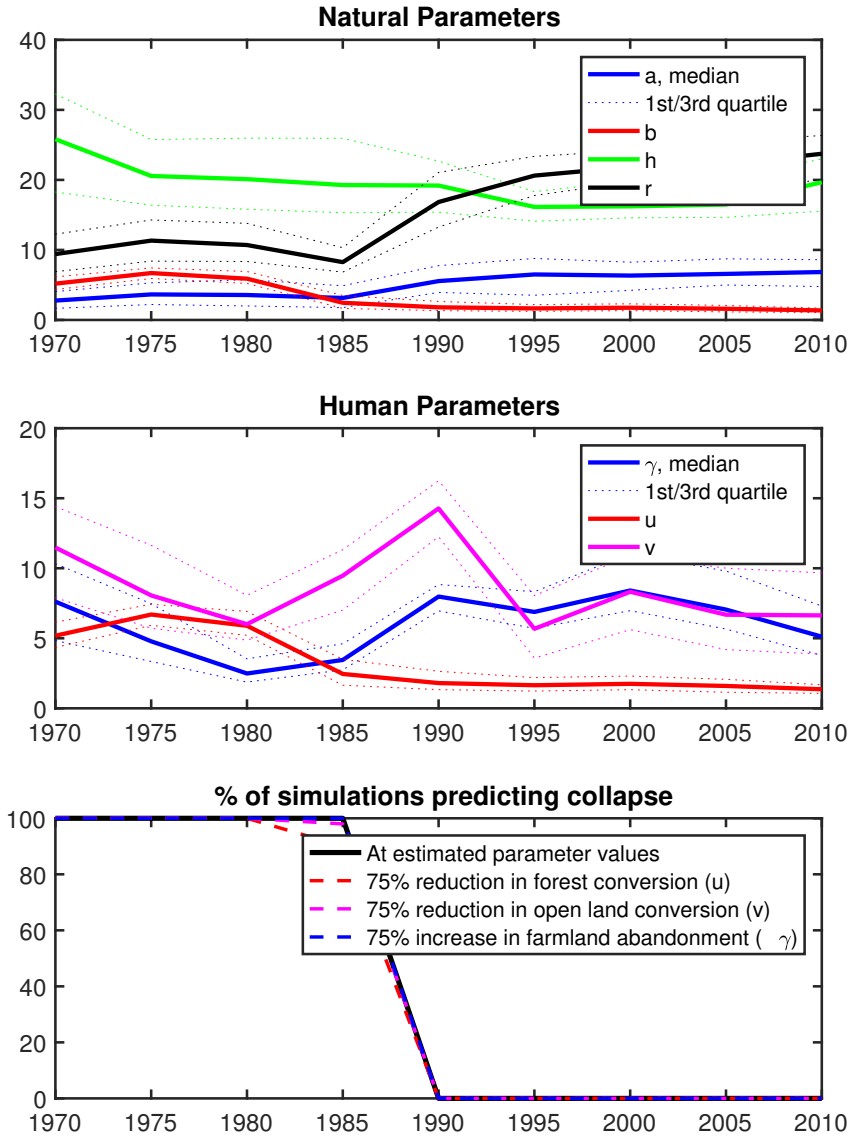

Figure A.17: Fitted discrete-time parameter ensembles for Costa Rica with 25% reduction. The upper and middle panels reproduce the results of Figure 4.5 though fitted over 10 years instead of 15, confirming that the results are not sensitive to the fitting window. The bottom subpanel shows that for a 75% change in parameters, reducing u still produces the best results.

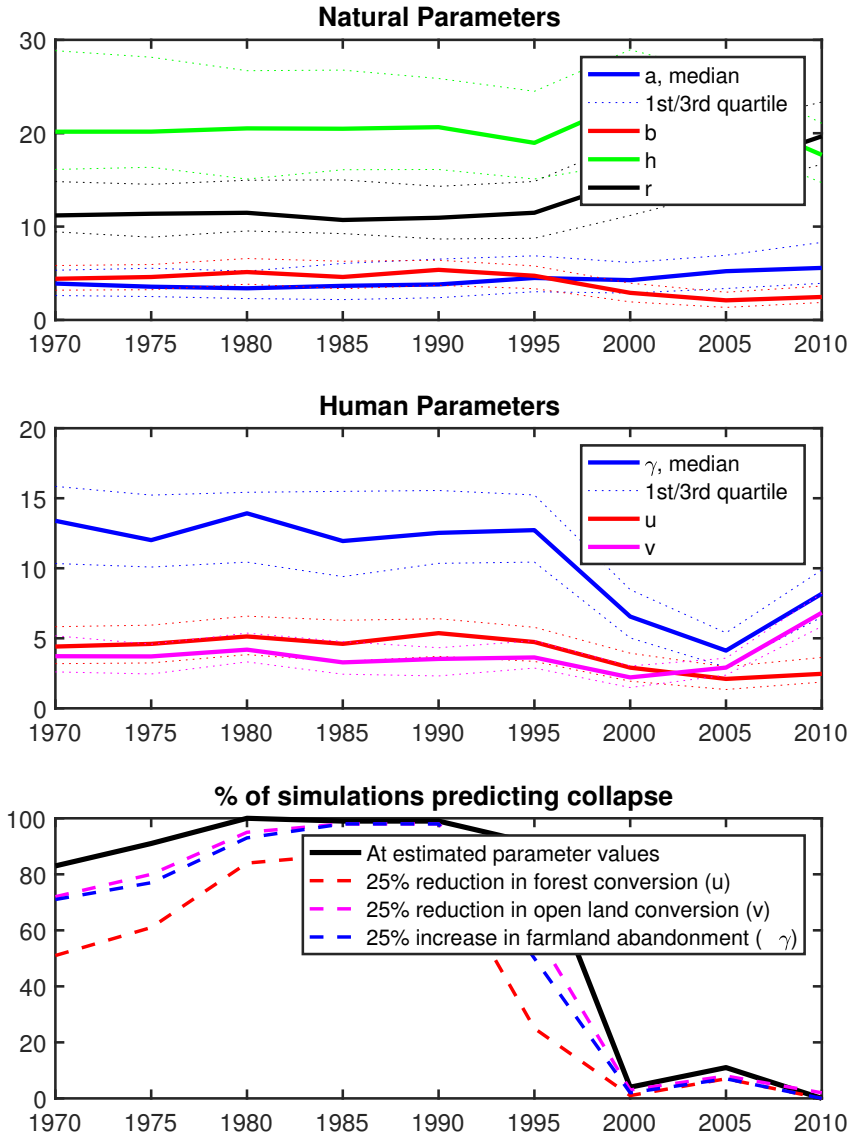

Figure A.18: Fitted discrete-time parameter ensembles for Vietnam with 25% reduction. The upper and middle panels reproduce the results of Figure 4.7 though fitted over 10 years instead of 15, confirming that the results are not sensitive to the fitting window. The bottom subpanel shows that for a 25% change in parameters, reducing u still produces the best results.

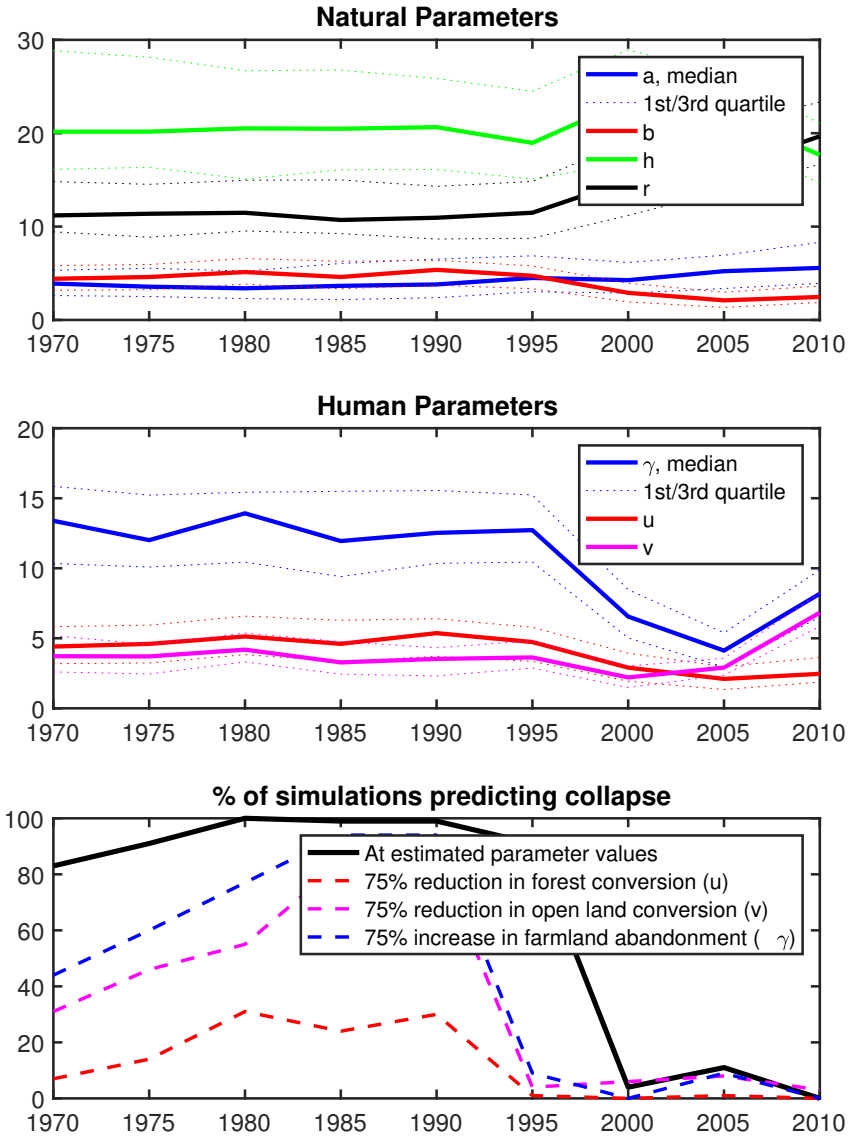

Figure A.19: Fitted discrete-time parameter ensembles for Vietnam with 25% reduction. The upper and middle panels reproduce the results of Figure 4.7 though fitted over 10 years instead of 15, confirming that the results are not sensitive to the fitting window. The bottom subpanel shows that for a 75% change in parameters, reducing u still produces the best results.